ASTRONOMY & ASTROPHYSICS
SUPPLEMENT SERIES

Astron. Astrophys. Suppl. Ser. **131**, 499–522 (1998)

Atomic data from the IRON Project

XXIX. Radiative rates for transitions within the $n = 2$ complex in ions of the boron isoelectronic sequence*

M.E. Galavís[1,2,3], C. Mendoza[2,3], and C.J. Zeippen[3]

[1] Departamento de Física, Universidad Metropolitana, PO Box 76819, Caracas 1070A, Venezuela
[2] Centro de Física, Instituto Venezolano de Investigaciones Científicas (IVIC), PO Box 21827, Caracas 1020A, Venezuela
[3] URA 173 (associée au CNRS et à l'Université Paris 7) et DAEC, Observatoire de Paris, F-92195 Meudon, France

Received December 30, 1997; accepted March 18, 1998

Abstract. As part of the IRON Project, radiative rates have been calculated for the E1, E2 and M1 transitions within the $n = 2$ complex in ions of the boron isoelectronic sequence ($6 \leq Z \leq 28$). The computations have been carried out with the atomic structure code SUPERSTRUCTURE which facilitates the generation of extended radiative datasets including configuration interaction, Breit–Pauli relativistic contributions and semi-empirical term-energy corrections. By means of extensive comparisons with the available datasets for this sequence, with detailed single-ion calculations and recent experiments, we have been able to assign accuracy ratings to the present A-values. We find that in general the spin-allowed and spin-forbidden E1 transitions are accurate to 10% and 20%, respectively, except for a few transitions in ions with $Z \leq 7$ that are perturbed by admixture with low-lying $n = 3$ states (e.g. $2s^2 3l$) and for those affected by the avoided crossing of the $2s2p^2\ ^2S_{1/2}$ and $^2P_{1/2}$ which takes place at $Z \sim 22$. It is concluded that, statistically, the present dataset is the most accurate to date for this astrophysically relevant sequence.

Key words: atomic data — atomic processes

1. Introduction

Transitions within the $n = 2$ complex of ions in the boron isoelectronic sequence are of great importance in the study of laboratory and astrophysical plasmas. Their spectral lines are observed in a wide variety of astronomical sources where they are frequently used as temperature, density and abundance diagnostics (Peng & Pradhan 1995). For example, lines belonging to C II, N III and O IV have been identified in the spectrum of planetary nebulae (Stencel et al. 1981), giant stars (Judge 1986a,b; Carpenter et al. 1991), symbiotic stars (Nussbaumer & Schild 1981; Hayes & Nussbaumer 1986), in the solar chromosphere (Doschek et al. 1977) and the solar transition region (Doschek et al. 1976; Brekke et al. 1991). Sandlin et al. (1976) have observed the five components of the $2s^2 2p\ ^2P^0 - 2s2p^2\ ^4P$ multiplet of Fe XXII in solar-flare spectra.

Reliable laboratory lifetime measurements based on the beam-foil excitation technique have been reported for the short-lived states of C II and N III (Reistad et al. 1986; Bengtsson et al. 1995; Nandi et al. 1996) and for the ^4P_J metastable levels of Fe XXII by Hutton et al. (1997). Also, by recording the spontaneous emission time from metastable ions stored in a cylindrical radio-frequency ion trap, Fang et al. (1993a,b) succeeded in determining radiative rates for the ^4P_J levels in C II and N III. These experimental data offer a good opportunity for comparison with theory.

Due to their importance in astronomy, ions of the boron sequence have received a high priority in the IRON Project (IP, see the general description by Hummer et al. 1993), an on-going international collaboration concerned with the computation of accurate atomic data for ions of astrophysical interest (a complete list of papers in the IP series can be found at the URL `http://www.am.qub.ac.uk/projects/iron/papers/papers.html`). In the context of the IP, electron impact excitation rates for boron-like ions have been calculated by Zhang et al. (1994) as a continuation to the work by Blum & Pradhan (1992) on C II, N III and O IV.

Send offprint requests to: C.J. Zeippen

* A detailed table of the present transition probabilities is available in electronic form from the CDS via anonymous ftp 130.79.128.5

Table 1. Scaling parameters λ_{nl} used to generate the orbitals for the B-like ions

Z	1s	2s	2p	3s	3p	3d
6	1.430	1.299	1.205	1.353	1.380	2.472
7	1.422	1.297	1.195	1.360	1.402	2.326
8	1.417	1.299	1.191	1.365	1.406	2.165
9	1.412	1.302	1.189	1.378	1.410	2.055
10	1.409	1.305	1.188	1.380	1.414	1.977
11	1.406	1.307	1.188	1.382	1.418	1.920
12	1.404	1.309	1.188	1.383	1.420	1.875
13	1.401	1.311	1.189	1.385	1.422	1.840
14	1.400	1.313	1.189	1.386	1.424	1.812
15	1.398	1.314	1.189	1.387	1.426	1.789
16	1.397	1.315	1.190	1.388	1.427	1.769
17	1.396	1.316	1.190	1.389	1.428	1.752
18	1.395	1.317	1.190	1.390	1.429	1.737
19	1.394	1.318	1.191	1.391	1.431	1.725
20	1.393	1.319	1.191	1.392	1.432	1.714
21	1.392	1.319	1.191	1.392	1.432	1.704
22	1.391	1.320	1.191	1.393	1.433	1.695
23	1.391	1.320	1.192	1.393	1.434	1.687
24	1.390	1.321	1.192	1.394	1.434	1.680
25	1.389	1.322	1.192	1.394	1.435	1.673
26	1.389	1.322	1.192	1.395	1.435	1.667
27	1.389	1.322	1.192	1.395	1.436	1.662
28	1.388	1.323	1.193	1.395	1.436	1.657

The present study can be regarded as a complement to this work by generating an accurate (∼10%, say) dataset containing the corresponding radiative-decay rates. It is primarily intended to increase the content and usefulness of the IP public databases, but an attempt has also been made to provide accuracy ratings for the listed transition probabilities.

Radiative datasets for the boron sequence have been previously computed by Dankwort & Trefftz (DT, 1978) in the multiconfiguration Hartree-Fock (MCHF) approximation; by Cheng et al. (CKD, 1979) using the multiconfiguration Dirac-Fock method; and by an approach based on many-body perturbation theory by Merkelis et al. (MVGK, 1995). These calculations are mainly concerned with electric dipole transitions (E1) although Cheng et al. have also considered the forbidden electric quadrupole (E2) and magnetic dipole (M1) transitions within the ground term. The latter transitions have also been calculated for the sequence by Froese Fischer (1983) in the MCHF approximation. The aim of the present work is to generate an A-value dataset for the $n = 2$ transitions in B-like ions more complete and of higher statistical accuracy than previous work. In this respect it is worth mentioning that the level of agreement between the published datasets is not satisfactory: for some transitions the quoted rates show discrepancies as large as an order of magnitude. We are therefore interested in establishing the physical effects that cause such differences. Since most of the problems appear towards the low-Z end of the sequence due to correlation effects, we make extensive comparisons with experiment and with the following detailed single-ion calculations: C II by Nussbaumer & Storey (1981), Lennon et al. (1985) and Froese Fischer (1994); N III by Nussbaumer & Storey (1979), Brage et al. (1995) and Bell et al. (1995); and O IV by Brage et al. (1996).

For the present work we have made use of the atomic structure program SUPERSTRUCTURE (Eissner et al. 1974; Nussbaumer & Storey 1978; Eissner 1991). This code allows for the inclusion of configuration interaction (CI) and Breit-Pauli (BP) relativistic effects, and has proven to be a practical platform for the computation of extended radiative datasets. Within the IP it has recently been used in a similar fashion for the carbon and oxygen isoelectronic sequences by Galavís et al. (1997).

The numerical method is described in Sect. 2, followed by analyses of the energy levels (Sect. 3) and transition probabilities (Sect. 4). Conclusions are summarised in Sect. 5.

2. Method

The calculations of the transition probabilities have been carried out with the computer program SUPERSTRUCTURE, originally developed by Eissner et al. (1974) and later modified by Nussbaumer & Storey (1978) to ensure greater flexibility in the radial orbital functions. The method has been summarized in our previous article (Galavís et al. 1997). As described by Eissner (1991) the LS terms are represented by CI wavefunctions of the type

$$\Psi = \sum_i \phi_i c_i \ , \tag{1}$$

where the configuration basis functions ϕ_i are constructed from one-electron spectroscopic orbitals $P(nl)$, generated within a statistical Thomas–Fermi–Dirac model potential $V(\lambda_{nl})$ (Eissner & Nussbaumer 1969). For the boron sequence we have adopted the 11-configuration basis set used by Biémont et al. (1994) for C II and N III, namely $2s^22p$, $2s2p^2$, $2p^3$, $2s^23s$, $2s^23p$, $2s^23d$, $2p^23d$, $2s3d^2$, 2s2p3s, 2s2p3p, 2s2p3d. To determine the scaling parameters λ_{nl}, a special optimization procedure described and discussed in detail by these authors is employed. It is found that the accuracy of the energy levels, and consequently that of the transition probabilities, depends strongly on how the optimization is performed. The variational procedure adopted here minimises with equal weights the sum of energies of all the terms in specific configurations, that is

$$\mathcal{F} = \sum_{i=1}^{N} E(S_i, L_i) \ . \tag{2}$$

More precisely, the 1s, 2s, 2p and 3s orbitals are first optimized with a functional $\mathcal{F}$ containing the energies of all terms in the $2s^22p$, $2s2p^2$, $2p^3$ and $2s^23s$ configurations.

Table 2. Experimental and calculated level energies (cm^{-1}) for the boron sequence. Expt: spectroscopic data by Moore (1970) for C II, Moore (1975) for N III and Edlén (1983) for the rest. Pres: present results. MVGK: Merkelis et al. (1995). CKD: Cheng et al. (1979)

Z	i	Level	Expt	Pres	MVGK	CKD	Z	i	Level	Expt	Pres	MVGK	CKD
6	1	$2s^22p\ ^2P^0_{1/2}$	0	0			9	1	$2s^22p\ ^2P^0_{1/2}$	0	0	0	0
	2	$2s^22p\ ^2P^0_{3/2}$	63	64				2	$2s^22p\ ^2P^0_{3/2}$	745	737	723	898
	3	$2s2p^2\ ^4P_{1/2}$	43003	39571				3	$2s2p^2\ ^4P_{1/2}$	85793	82203	84946	80464
	4	$2s2p^2\ ^4P_{3/2}$	43025	39594				4	$2s2p^2\ ^4P_{3/2}$	86045	82459	85198	80714
	5	$2s2p^2\ ^4P_{5/2}$	43054	39623				5	$2s2p^2\ ^4P_{5/2}$	86409	82827	85554	81070
	6	$2s2p^2\ ^2D_{5/2}$	74930	77499				6	$2s2p^2\ ^2D_{5/2}$	152874	157135	149387	159453
	7	$2s2p^2\ ^2D_{3/2}$	74933	77501				7	$2s2p^2\ ^2D_{3/2}$	152897	157147	149407	159432
	8	$2s2p^2\ ^2S_{1/2}$	96494	101172				8	$2s2p^2\ ^2S_{1/2}$	197563	202664	194725	202771
	9	$2s2p^2\ ^2P_{1/2}$	110624	116737				9	$2s2p^2\ ^2P_{1/2}$	214878	223702	214219	226744
	10	$2s2p^2\ ^2P_{3/2}$	110666	116777				10	$2s2p^2\ ^2P_{3/2}$	215349	224165	214673	227221
	11	$2p^3\ ^4S^0_{3/2}$	142027	142394				11	$2p^3\ ^4S^0_{3/2}$	276416	277167	275147	274697
	12	$2p^3\ ^2D^0_{5/2}$	150462	153635				12	$2p^3\ ^2D^0_{5/2}$	307226	314794	299284	318230
	13	$2p^3\ ^2D^0_{3/2}$	150467	153641				13	$2p^3\ ^2D^0_{3/2}$	307274	314853	299348	318283
	14	$2p^3\ ^2P^0_{1/2}$	168730	174646				14	$2p^3\ ^2P^0_{1/2}$	347421	358289	340540	359681
	15	$2p^3\ ^2P^0_{3/2}$	168748	174662				15	$2p^3\ ^2P^0_{3/2}$	347439	358300	340548	359816
7	1	$2s^22p\ ^2P^0_{1/2}$	0	0		0	10	1	$2s^22p\ ^2P^0_{1/2}$	0	0	0	0
	2	$2s^22p\ ^2P^0_{3/2}$	174	174		333		2	$2s^22p\ ^2P^0_{3/2}$	1308	1292	1275	1465
	3	$2s2p^2\ ^4P_{1/2}$	57187	53769		52202		3	$2s2p^2\ ^4P_{1/2}$	100298	96647	99644	94846
	4	$2s2p^2\ ^4P_{3/2}$	57247	53830		52260		4	$2s2p^2\ ^4P_{3/2}$	100742	97098	100090	95287
	5	$2s2p^2\ ^4P_{5/2}$	57328	53912		52337		5	$2s2p^2\ ^4P_{5/2}$	101390	97751	100729	95924
	6	$2s2p^2\ ^2D_{5/2}$	101024	104526		107601		6	$2s2p^2\ ^2D_{5/2}$	178992	183397	176220	185558
	7	$2s2p^2\ ^2D_{3/2}$	101031	104530		107537		7	$2s2p^2\ ^2D_{3/2}$	179022	183412	176245	185552
	8	$2s2p^2\ ^2S_{1/2}$	131004	135842		136605		8	$2s2p^2\ ^2S_{1/2}$	230855	236008	228429	235977
	9	$2s2p^2\ ^2P_{1/2}$	145876	153264		157271		9	$2s2p^2\ ^2P_{1/2}$	249281	258431	248748	261298
	10	$2s2p^2\ ^2P_{3/2}$	145986	153373		157404		10	$2s2p^2\ ^2P_{3/2}$	250109	259241	249546	262120
	11	$2p^3\ ^4S^0_{3/2}$	186797	187418		185069		11	$2p^3\ ^4S^0_{3/2}$	321617	322415	320560	319894
	12	$2p^3\ ^2D^0_{5/2}$	203075	208844		214486		12	$2p^3\ ^2D^0_{5/2}$	359543	367443	353281	370440
	13	$2p^3\ ^2D^0_{3/2}$	203089	208863		214501		13	$2p^3\ ^2D^0_{3/2}$	359612	367527	353372	370517
	14	$2p^3\ ^2P^0_{1/2}$	230404	239517		243115		14	$2p^3\ ^2P^0_{1/2}$	406008	417197	400506	418199
	15	$2p^3\ ^2P^0_{3/2}$	230409	239520		243260		15	$2p^3\ ^2P^0_{3/2}$	406053	417228	400534	418352
8	1	$2s^22p\ ^2P^0_{1/2}$	0	0	0	0	11	1	$2s^22p\ ^2P^0_{1/2}$	0	0	0	0
	2	$2s^22p\ ^2P^0_{3/2}$	386	383	372	536		2	$2s^22p\ ^2P^0_{3/2}$	2135	2110	2089	2299
	3	$2s2p^2\ ^4P_{1/2}$	71440	67925	70106	66259		3	$2s2p^2\ ^4P_{1/2}$	115004	111311	114476	109453
	4	$2s2p^2\ ^4P_{3/2}$	71571	68059	70235	66388		4	$2s2p^2\ ^4P_{3/2}$	115735	112050	115210	110179
	5	$2s2p^2\ ^4P_{5/2}$	71755	68246	70413	66567		5	$2s2p^2\ ^4P_{5/2}$	116806	113129	116272	111235
	6	$2s2p^2\ ^2D_{5/2}$	126936	130936	121908	133515		6	$2s2p^2\ ^2D_{5/2}$	205415	209910	203084	211961
	7	$2s2p^2\ ^2D_{3/2}$	126950	130945	121923	133476		7	$2s2p^2\ ^2D_{3/2}$	205452	209923	203110	211968
	8	$2s2p^2\ ^2S_{1/2}$	164366	169367	160426	169701		8	$2s2p^2\ ^2S_{1/2}$	264396	269570	262199	269456
	9	$2s2p^2\ ^2P_{1/2}$	180481	188768	179375	192144		9	$2s2p^2\ ^2P_{1/2}$	283848	293192	283346	295970
	10	$2s2p^2\ ^2P_{3/2}$	180722	189008	179608	192401		10	$2s2p^2\ ^2P_{3/2}$	285183	294506	284642	297296
	11	$2p^3\ ^4S^0_{3/2}$	231537	232226	229755	229813		11	$2p^3\ ^4S^0_{3/2}$	367314	368150	366392	365585
	12	$2p^3\ ^2D^0_{5/2}$	255155	262131	243729	266306		12	$2p^3\ ^2D^0_{5/2}$	412315	420421	407095	423127
	13	$2p^3\ ^2D^0_{3/2}$	255184	262167	243770	266338		13	$2p^3\ ^2D^0_{3/2}$	412401	420528	407209	423225
	14	$2p^3\ ^2P^0_{1/2}$	289017	299326	278883	301393		14	$2p^3\ ^2P^0_{1/2}$	465019	476399	460331	477155
	15	$2p^3\ ^2P^0_{3/2}$	289024	299328	278883	301526		15	$2p^3\ ^2P^0_{3/2}$	465116	476473	460404	477351

Then the 3p and the 3d orbitals are determined by including in $\mathcal{F}$ all the terms in the $2s^22p$, $2s2p^2$, $2p^3$, $2s^23s$, $2s^23p$ and $2s^23d$ configurations. Finally, the 3s function is reoptimized with the states generated by the 2s2p3s configuration so as to obtain a slight improvement in the term energies. The final scaling parameters are listed in Table 1.

In SUPERSTRUCTURE the Hamiltonian is taken to be of the form

$$H = H_{\rm nr} + H_{\rm bp} \quad (3)$$

where $H_{\rm nr}$ is the usual non-relativistic Hamiltonian. The relativistic corrections $H_{\rm bp}$ are taken into account through the Breit-Pauli (BP) aproximation (Jones 1970, 1971): the one-body terms which include the mass-variation correction, the Darwin term and the spin-orbit interaction; and the two-body fine-structure terms, namely the spin-spin and spin-other-orbit interactions. Using perturbation

Table 2. continued

Z	i	Level	Expt	Pres	MVGK	CKD	Z	i	Level	Expt	Pres	MVGK	CKD
12	1	$2s^22p\ ^2P^0_{1/2}$	0	0	0	0	15	1	$2s^22p\ ^2P^0_{1/2}$	0	0	0	0
	2	$2s^22p\ ^2P^0_{3/2}$	3302	3263	3239	3471		2	$2s^22p\ ^2P^0_{3/2}$	9703	9585	9546	9871
	3	$2s2p^2\ ^4P_{1/2}$	129979	126254	129546	124341		3	$2s2p^2\ ^4P_{1/2}$	177187	173427	176965	171345
	4	$2s2p^2\ ^4P_{3/2}$	131120	127406	130693	125475		4	$2s2p^2\ ^4P_{3/2}$	180671	176919	180459	174804
	5	$2s2p^2\ ^4P_{5/2}$	132792	129085	132353	127127		5	$2s2p^2\ ^4P_{5/2}$	185634	181993	185397	179737
	6	$2s2p^2\ ^2D_{5/2}$	232275	236828	230252	238793		6	$2s2p^2\ ^2D_{3/2}$	316792	321328	315239	323172
	7	$2s2p^2\ ^2D_{3/2}$	232313	236830	230269	238806		7	$2s2p^2\ ^2D_{5/2}$	316899	321514	315414	323277
	8	$2s2p^2\ ^2S_{1/2}$	298302	303486	296259	303331		8	$2s2p^2\ ^2S_{1/2}$	403246	408468	401413	408450
	9	$2s2p^2\ ^2P_{1/2}$	318732	328164	318200	330909		9	$2s2p^2\ ^2P_{1/2}$	426896	436074	426016	438907
	10	$2s2p^2\ ^2P_{3/2}$	320747	330170	320177	332928		10	$2s2p^2\ ^2P_{3/2}$	432117	441463	431242	444351
	11	$2p^3\ ^4S^0_{3/2}$	413700	414557	412869	411958		11	$2p^3\ ^4S^0_{3/2}$	558955	559796	558228	557160
	12	$2p^3\ ^2D^0_{5/2}$	465750	473989	461254	476484		12	$2p^3\ ^2D^0_{3/2}$	631974	640428	628788	642527
	13	$2p^3\ ^2D^0_{3/2}$	465839	474107	461378	476591		13	$2p^3\ ^2D^0_{5/2}$	632177	640556	628934	642681
	14	$2p^3\ ^2P^0_{1/2}$	524669	536156	520524	536752		14	$2p^3\ ^2P^0_{1/2}$	709620	721095	706305	721525
	15	$2p^3\ ^2P^0_{3/2}$	524862	536314	520684	537034		15	$2p^3\ ^2P^0_{3/2}$	710703	722070	707327	722648
13	1	$2s^22p\ ^2P^0_{1/2}$	0	0	0	0	16	1	$2s^22p\ ^2P^0_{1/2}$	0	0	0	0
	2	$2s^22p\ ^2P^0_{3/2}$	4890	4832	4804	5061		2	$2s^22p\ ^2P^0_{3/2}$	13136	12975	12926	13299
	3	$2s2p^2\ ^4P_{1/2}$	145288	141542	144935	139575		3	$2s2p^2\ ^4P_{1/2}$	193920	190163	193749	188021
	4	$2s2p^2\ ^4P_{3/2}$	146998	143263	146651	141272		4	$2s2p^2\ ^4P_{3/2}$	198713	194958	198551	192780
	5	$2s2p^2\ ^4P_{5/2}$	149488	145762	149127	143739		5	$2s2p^2\ ^4P_{5/2}$	205426	201683	205231	199464
	6	$2s2p^2\ ^2D_{3/2}$	259733	264274	257905	266195		6	$2s2p^2\ ^2D_{3/2}$	346716	351229	345241	353048
	7	$2s2p^2\ ^2D_{5/2}$	259711	264299	257915	266191		7	$2s2p^2\ ^2D_{5/2}$	346981	351592	345599	353296
	8	$2s2p^2\ ^2S_{1/2}$	332685	337877	330748	337720		8	$2s2p^2\ ^2S_{1/2}$	439562	444805	437708	444955
	9	$2s2p^2\ ^2P_{1/2}$	354082	363512	353473	366262		9	$2s2p^2\ ^2P_{1/2}$	464807	473734	463745	476634
	10	$2s2p^2\ ^2P_{3/2}$	356972	366424	356334	369193		10	$2s2p^2\ ^2P_{3/2}$	471431	480644	470379	483642
	11	$2p^3\ ^4S^0_{3/2}$	460965	461828	460197	459208		11	$2p^3\ ^4S^0_{3/2}$	610113	610915	609357	608298
	12	$2p^3\ ^2D^0_{5/2}$	520058	528378	516096	530717		12	$2p^3\ ^2D^0_{3/2}$	689936	698399	686989	700425
	13	$2p^3\ ^2D^0_{3/2}$	520119	528480	516200	530804		13	$2p^3\ ^2D^0_{5/2}$	690465	698826	687455	700887
	14	$2p^3\ ^2P^0_{1/2}$	585171	596704	581408	597199		14	$2p^3\ ^2P^0_{1/2}$	774040	785419	770827	785877
	15	$2p^3\ ^2P^0_{3/2}$	585531	597011	581725	597635		15	$2p^3\ ^2P^0_{3/2}$	775815	787042	772534	787665
14	1	$2s^22p\ ^2P^0_{1/2}$	0	0	0	0	17	1	$2s^22p\ ^2P^0_{1/2}$	0	0	0	0
	2	$2s^22p\ ^2P^0_{3/2}$	6990	6907	6874	7161		2	$2s^22p\ ^2P^0_{3/2}$	17410	17192	17130	17564
	3	$2s2p^2\ ^4P_{1/2}$	161001	157244	160718	155219		3	$2s2p^2\ ^4P_{1/2}$	211267	207520	211137	205318
	4	$2s2p^2\ ^4P_{3/2}$	163476	159728	163201	157677		4	$2s2p^2\ ^4P_{3/2}$	217736	213979	217610	211738
	5	$2s2p^2\ ^4P_{5/2}$	167047	163310	166754	161221		5	$2s2p^2\ ^4P_{5/2}$	226609	222864	226436	220585
	6	$2s2p^2\ ^2D_{3/2}$	287846	292392	286178	294271		6	$2s2p^2\ ^2D_{3/2}$	377773	382247	376337	384051
	7	$2s2p^2\ ^2D_{5/2}$	287866	292473	286245	294300		7	$2s2p^2\ ^2D_{5/2}$	378306	382897	376991	384546
	8	$2s2p^2\ ^2S_{1/2}$	367640	372843	365775	372729		8	$2s2p^2\ ^2S_{1/2}$	476617	481883	474678	482284
	9	$2s2p^2\ ^2P_{1/2}$	390068	399416	389343	402196		9	$2s2p^2\ ^2P_{1/2}$	504099	512688	502828	515667
	10	$2s2p^2\ ^2P_{3/2}$	394031	403458	393294	406270		10	$2s2p^2\ ^2P_{3/2}$	512198	521224	510919	524368
	11	$2p^3\ ^4S^0_{3/2}$	509314	510174	508580	507538		11	$2p^3\ ^4S^0_{3/2}$	663014	663758	662188	661183
	12	$2p^3\ ^2D^0_{5/2}$	575457	583822	571902	586040		12	$2p^3\ ^2D^0_{3/2}$	749516	757964	746734	759939
	13	$2p^3\ ^2D^0_{3/2}$	575430	583853	571928	586052		13	$2p^3\ ^2D^0_{5/2}$	750581	758894	747731	760918
	14	$2p^3\ ^2P^0_{1/2}$	646744	658272	643250	658714		14	$2p^3\ ^2P^0_{1/2}$	840265	851500	837080	852030
	15	$2p^3\ ^2P^0_{3/2}$	647381	658833	643835	659412		15	$2p^3\ ^2P^0_{3/2}$	843080	854106	839820	854825

theory, the relativistic wavefunction $\psi_i^{\rm r}$ can be expanded in terms of the non-relativistic functions $\psi_j^{\rm nr}$:

$$\psi_i^{\rm r} = \psi_i^{\rm nr} + \sum_{j\neq i} \psi_j^{\rm nr} \times \frac{< \psi_j^{\rm nr}|H_{\rm bp}|\psi_i^{\rm nr} >}{E_i^{\rm nr} - E_j^{\rm nr}} + \ldots \qquad (4)$$

Small fractional errors in the non-relativistic energies $E_i^{\rm nr}$ and $E_j^{\rm nr}$ can lead to much larger errors in the differences $E_i^{\rm nr} - E_j^{\rm nr}$ for $j \neq i$. Therefore, by using accurate experimental level energies by Moore (1970, 1975) and Edlén (1983), improved estimates of the non-relativistic energies are obtained and a modified $H_{\rm nr}$ is constructed. This semi-empirical term energy correction (TEC) procedure was originally implemented in SUPERSTRUCTURE by Zeippen et al. (1977).

In the present case, for ions with $Z \geq 8$, corrections are made so as to shift the computed excitation energy of the lowest level in each of the 8 terms in the $n = 2$ complex to its observed value. For C II and N III, due to the mixture with low $n = 3$ states, additional terms arising from configurations of the type $2s^23l$ and $2s2p3l$ are also corrected.

Table 2. continued

Z	i	Level	Expt	Pres	MVGK	CKD	Z	i	Level	Expt	Pres	MVGK	CKD
18	1	2s^{2}2p ^{2}P$^0_{1/2}$	0	0		0	21	1	2s^{2}2p ^{2}P$^0_{1/2}$	0	0		0
	2	2s^{2}2p ^{2}P$^0_{3/2}$	22653	22362		22795		2	2s^{2}2p ^{2}P$^0_{3/2}$	45634	44978		45712
	3	2s2p^2 ^{4}P$_{1/2}$	229299	225566		223304		3	2s2p^2 ^{4}P$_{1/2}$	288130	284453		281969
	4	2s2p^2 ^{4}P$_{3/2}$	237886	234125		231823		4	2s2p^2 ^{4}P$_{3/2}$	306682	302855		300361
	5	2s2p^2 ^{4}P$_{5/2}$	249376	245628		243297		5	2s2p^2 ^{4}P$_{5/2}$	329224	325402		322960
	6	2s2p^2 ^{2}D$_{3/2}$	410124	414542		416345		6	2s2p^2 ^{2}D$_{3/2}$	516632	520745		522607
	7	2s2p^2 ^{2}D$_{5/2}$	411084	415635		417236		7	2s2p^2 ^{2}D$_{5/2}$	520582	524827		526313
	8	2s2p^2 ^{2}S$_{1/2}$	514414	519708		520451		8	2s2p^2 ^{2}S$_{1/2}$	632376	637880		639969
	9	2s2p^2 ^{2}P$_{1/2}$	545109	553277		556340		9	2s2p^2 ^{2}P$_{1/2}$	682185	688536		691891
	10	2s2p^2 ^{2}P$_{3/2}$	554656	563439		566772		10	2s2p^2 ^{2}P$_{3/2}$	694949	702600		706749
	11	2p^3 ^{4}S$^0_{3/2}$	717895	718557		716054		11	2p^3 ^{4}S$^0_{3/2}$	896804	897051		894958
	12	2p^3 ^{2}D$^0_{3/2}$	810913	819317		821268		12	2p^3 ^{2}D$^0_{3/2}$	1008060	1016110		1018125
	13	2p^3 ^{2}D$^0_{5/2}$	812807	821036		823056		13	2p^3 ^{2}D$^0_{5/2}$	1015224	1022915		1025128
	14	2p^3 ^{2}P$^0_{1/2}$	908573	919614		920264		14	2p^3 ^{2}P$^0_{1/2}$	1129044	1139125		1140449
	15	2p^3 ^{2}P$^0_{3/2}$	912906	923661		924533		15	2p^3 ^{2}P$^0_{3/2}$	1142543	1151933		1153681
19	1	2s^{2}2p ^{2}P$^0_{1/2}$	0	0		0	22	1	2s^{2}2p ^{2}P$^0_{1/2}$	0	0	0	0
	2	2s^{2}2p ^{2}P$^0_{3/2}$	29004	28618		29130		2	2s^{2}2p ^{2}P$^0_{3/2}$	56240	55397	55161	56287
	3	2s2p^2 ^{4}P$_{1/2}$	248081	244366		242047		3	2s2p^2 ^{4}P$_{1/2}$	309494	305837	309218	303272
	4	2s2p^2 ^{4}P$_{3/2}$	259315	255545		253189		4	2s2p^2 ^{4}P$_{3/2}$	332976	329091	332546	326546
	5	2s2p^2 ^{4}P$_{5/2}$	273929	270170		267802		5	2s2p^2 ^{4}P$_{5/2}$	360386	356503	358711	354062
	6	2s2p^2 ^{2}D$_{3/2}$	443935	448276		450097		6	2s2p^2 ^{2}D$_{3/2}$	555879	559829	553867	561754
	7	2s2p^2 ^{2}D$_{5/2}$	445548	450031		451599		7	2s2p^2 ^{2}D$_{5/2}$	561756	565807	560009	567289
	8	2s2p^2 ^{2}S$_{1/2}$	552948	558285		559455		8	2s2p^2 ^{2}S$_{1/2}$	673607	679110	670674	681673
	9	2s2p^2 ^{2}P$_{1/2}$	588210	595867		599028		9	2s2p^2 ^{2}P$_{1/2}$	733766	739321	730420	742849
	10	2s2p^2 ^{2}P$_{3/2}$	599072	607547		611121		10	2s2p^2 ^{2}P$_{3/2}$	747063	754179	743565	758716
	11	2p^3 ^{4}S$^0_{3/2}$	774994	775549		773158		11	2p^3 ^{4}S$^0_{3/2}$	961979	962017	959730	960163
	12	2p^3 ^{2}D$^0_{3/2}$	874326	882654		884614		12	2p^3 ^{2}D$^0_{3/2}$	1078865	1086689	1075608	1088799
	13	2p^3 ^{2}D$^0_{5/2}$	877443	885543		887602		13	2p^3 ^{2}D$^0_{5/2}$	1089065	1096453	1085703	1098836
	14	2p^3 ^{2}P$^0_{1/2}$	979260	990047		990878		14	2p^3 ^{2}P$^0_{1/2}$	1208833	1218438	1204400	1220131
	15	2p^3 ^{2}P$^0_{3/2}$	985749	996149		997249		15	2p^3 ^{2}P$^0_{3/2}$	1227640	1236330	1223024	1238571
20	1	2s^{2}2p ^{2}P$^0_{1/2}$	0	0	0	0	23	1	2s^{2}2p ^{2}P$^0_{1/2}$	0	0		0
	2	2s^{2}2p ^{2}P$^0_{3/2}$	36611	36107	35971	36717		2	2s^{2}2p ^{2}P$^0_{3/2}$	68609	67534		68618
	3	2s2p^2 ^{4}P$_{1/2}$	267675	263978	267549	261607		3	2s2p^2 ^{4}P$_{1/2}$	331800	328161		325490
	4	2s2p^2 ^{4}P$_{3/2}$	282190	278399	282016	276000		4	2s2p^2 ^{4}P$_{3/2}$	361262	357291		354686
	5	2s2p^2 ^{4}P$_{5/2}$	300475	296693	300171	294308		5	2s2p^2 ^{4}P$_{5/2}$	394170	390195		387763
	6	2s2p^2 ^{2}D$_{3/2}$	479378	483620	477784	485484		6	2s2p^2 ^{2}D$_{3/2}$	597308	601051		603049
	7	2s2p^2 ^{2}D$_{5/2}$	481952	486337	480574	487889		7	2s2p^2 ^{2}D$_{5/2}$	605828	609611		611099
	8	2s2p^2 ^{2}S$_{1/2}$	592229	597648	589771	599304		8	2s2p^2 ^{2}S$_{1/2}$	716100	721509		724517
	9	2s2p^2 ^{2}P$_{1/2}$	633779	640834	631598	644114		9	2s2p^2 ^{2}P$_{1/2}$	788853	793535		797291
	10	2s2p^2 ^{2}P$_{3/2}$	645731	653833	643394	657706		10	2s2p^2 ^{2}P$_{3/2}$	802445	808926		813911
	11	2p^3 ^{4}S$^0_{3/2}$	834552	834968	833148	832739		11	2p^3 ^{4}S$^0_{3/2}$	1030284	1030077		1028483
	12	2p^3 ^{2}D$^0_{3/2}$	939965	948179	937191	950186		12	2p^3 ^{2}D$^0_{3/2}$	1152684	1160200		1162413
	13	2p^3 ^{2}D$^0_{5/2}$	944802	952727	941951	954873		13	2p^3 ^{2}D$^0_{5/2}$	1166706	1173705		1176291
	14	2p^3 ^{2}P$^0_{1/2}$	1052638	1063110	1049030	1064189		14	2p^3 ^{2}P$^0_{1/2}$	1292383	1301410		1303526
	15	2p^3 ^{2}P$^0_{3/2}$	1062111	1072063	1058401	1073476		15	2p^3 ^{2}P$^0_{3/2}$	1318036	1325856		1328690

The radiative rates for electric dipole (E1), electric quadrupole (E2) and magnetic dipole (M1) transitions are respectively given by the expressions

$$A_{ij}(\mathrm{E1}) = 2.6774\ 10^9 (E_i - E_j)^3 \frac{1}{g_i} S_{ij}^{E1} \qquad (\mathrm{s}^{-1})\ , \qquad (5)$$

$$A_{ij}(\mathrm{E2}) = 2.6733\ 10^3 (E_i - E_j)^5 \frac{1}{g_i} S_{ij}^{E2} \qquad (\mathrm{s}^{-1})\ , \qquad (6)$$

and

$$A_{ij}(\mathrm{M1}) = 3.5644\ 10^4 (E_i - E_j)^3 \frac{1}{g_i} S_{ij}^{M1} \qquad (\mathrm{s}^{-1})\ . \qquad (7)$$

Here g_i is the statistical weight of the upper initial level i and energies E are expressed in Rydbergs. It is clear that the accuracy of the calculated A-values depends primarily on the quality of the wavefunctions used in evaluating the line strengths S_{ij}. However, relatively small errors in the energy difference $(E_i - E_j)$ are amplified by the large exponents in Eqs. ((5)–(7)). As shown, for example, by Galavís et al. (1997), in order to ensure an acceptable degree of accuracy the transition probabilities must be computed with an accurate and consistent dataset of experimental

Table 2. continued

Z	i	Level	Expt	Pres	MVGK	CKD
24	1	$2s^22p\ ^2P^0_{1/2}$	0	0	0	0
	2	$2s^22p\ ^2P^0_{3/2}$	82933	81572	81166	82897
	3	$2s2p^2\ ^4P_{1/2}$	355070	351451	354455	348653
	4	$2s2p^2\ ^4P_{3/2}$	391743	387654	390759	384990
	5	$2s2p^2\ ^4P_{5/2}$	430778	426681	429361	424276
	6	$2s2p^2\ ^2D_{3/2}$	641109	644601	638307	646692
	7	$2s2p^2\ ^2D_{5/2}$	653186	656618	650621	658135
	8	$2s2p^2\ ^2S_{1/2}$	760074	765285	756279	768720
	9	$2s2p^2\ ^2P_{1/2}$	847763	851545	842694	855604
	10	$2s2p^2\ ^2P_{3/2}$	861493	867235	856287	872738
	11	$2p^3\ ^4S^0_{3/2}$	1101907	1101425	1098265	1100136
	12	$2p^3\ ^2D^0_{3/2}$	1229877	1236988	1225607	1239336
	13	$2p^3\ ^2D^0_{5/2}$	1248550	1255066	1244077	1257914
	14	$2p^3\ ^2P^0_{1/2}$	1380094	1388436	1374205	1391053
	15	$2p^3\ ^2P^0_{3/2}$	1414392	1421156	1408067	1424717
25	1	$2s^22p\ ^2P^0_{1/2}$	0	0		0
	2	$2s^22p\ ^2P^0_{3/2}$	99412	97700		99322
	3	$2s2p^2\ ^4P_{1/2}$	379316	375718		372764
	4	$2s2p^2\ ^4P_{3/2}$	424634	420383		417663
	5	$2s2p^2\ ^4P_{5/2}$	470410	466147		463793
	6	$2s2p^2\ ^2D_{3/2}$	687478	690664		692873
	7	$2s2p^2\ ^2D_{5/2}$	704262	707231		708816
	8	$2s2p^2\ ^2S_{1/2}$	805750	810657		814510
	9	$2s2p^2\ ^2P_{1/2}$	910801	913723		918180
	10	$2s2p^2\ ^2P_{3/2}$	924638	929510		935621
	11	$2p^3\ ^4S^0_{3/2}$	1177003	1176215		1175274
	12	$2p^3\ ^2D^0_{3/2}$	1310878	1317450		1319978
	13	$2p^3\ ^2D^0_{5/2}$	1335017	1340933		1344116
	14	$2p^3\ ^2P^0_{1/2}$	1472385	1479908		1483126
	15	$2p^3\ ^2P^0_{3/2}$	1517398	1522872		1527331
26	1	$2s^22p\ ^2P^0_{1/2}$	0	0	0	0
	2	$2s^22p\ ^2P^0_{3/2}$	118260	116122	115443	118104
	3	$2s2p^2\ ^4P_{1/2}$	404535	400953	403328	397791
	4	$2s2p^2\ ^4P_{3/2}$	460158	455688	458172	452896
	5	$2s2p^2\ ^4P_{5/2}$	513252	508772	510567	506473
	6	$2s2p^2\ ^2D_{3/2}$	736621	739430	732518	741763
	7	$2s2p^2\ ^2D_{5/2}$	759534	761899	755453	763578
	8	$2s2p^2\ ^2S_{1/2}$	853392	857865	848212	862111
	9	$2s2p^2\ ^2P_{1/2}$	978322	980475	971284	985413
	10	$2s2p^2\ ^2P_{3/2}$	992338	996192	984644	1002981
	11	$2p^3\ ^4S^0_{3/2}$	1255684	1254559	1249923	1253990
	12	$2p^3\ ^2D^0_{3/2}$	1396208	1402053	1390162	1404805
	13	$2p^3\ ^2D^0_{5/2}$	1426557	1431722	1420124	1435308
	14	$2p^3\ ^2P^0_{1/2}$	1569707	1576247	1561491	1580153
	15	$2p^3\ ^2P^0_{3/2}$	1627775	1631675	1618534	1637210
27	1	$2s^22p\ ^2P^0_{1/2}$	0	0		0
	2	$2s^22p\ ^2P^0_{3/2}$	139702	137045		139472
	3	$2s2p^2\ ^4P_{1/2}$	430709	427153		423706
	4	$2s2p^2\ ^4P_{3/2}$	498549	493801		490911
	5	$2s2p^2\ ^4P_{5/2}$	559483	554738		552486
	6	$2s2p^2\ ^2D_{3/2}$	788745	791110		793569
	7	$2s2p^2\ ^2D_{5/2}$	819526	821122		822930
	8	$2s2p^2\ ^2S_{1/2}$	903288	907186		911803
	9	$2s2p^2\ ^2P_{1/2}$	1050742	1052247		1057762
	10	$2s2p^2\ ^2P_{3/2}$	1065079	1067763		1075319
	11	$2p^3\ ^4S^0_{3/2}$	1338022	1336582		1336298
	12	$2p^3\ ^2D^0_{3/2}$	1486474	1491389		1494325
	13	$2p^3\ ^2D^0_{5/2}$	1523638	1527913		1531885
	14	$2p^3\ ^2P^0_{1/2}$	1672526	1677930		1682534
	15	$2p^3\ ^2P^0_{3/2}$	1746262	1748288		1755019
28	1	$2s^22p\ ^2P^0_{1/2}$	0	0		0
	2	$2s^22p\ ^2P^0_{3/2}$	163975	160697		163657
	3	$2s2p^2\ ^4P_{1/2}$	457812	454281		450571
	4	$2s2p^2\ ^4P_{3/2}$	540056	534950		532043
	5	$2s2p^2\ ^4P_{5/2}$	609274	604203		602095
	6	$2s2p^2\ ^2D_{3/2}$	844069	845901		848598
	7	$2s2p^2\ ^2D_{5/2}$	884807	885421		887519
	8	$2s2p^2\ ^2S_{1/2}$	955750	958880		963968
	9	$2s2p^2\ ^2P_{1/2}$	1128525	1129491		1135801
	10	$2s2p^2\ ^2P_{3/2}$	1143381	1144698		1153238
	11	$2p^3\ ^4S^0_{3/2}$	1424051	1422296		1422477
	12	$2p^3\ ^2D^0_{3/2}$	1582371	1586046		1589433
	13	$2p^3\ ^2D^0_{5/2}$	1626755	1629933		1634567
	14	$2p^3\ ^2P^0_{1/2}$	1781337	1785387		1790989
	15	$2p^3\ ^2P^0_{3/2}$	1873629	1873396		1881751

energy levels. For the boron sequence, the work of Moore (1970, 1975) and Edlén (1983) is fully used.

3. Energy levels

Since the accuracy of the computed level energies gives a first indication of the quality of the wavefunctions, we make a detailed comparison with experiment and other calculations. Our aim is to obtain level energies to an accuracy of 5% or better and to be able to reproduce adequately the characteristic spectral features of the sequence. Present results are compared with the spectroscopic values, MVGK and CKD in Table 2 and in the histograms shown in Fig. 1. Apart from the $^2P^0_{1/2}$ ground levels, the present dataset contains 322 levels for $Z = 6 - 28$ of which 97% agree with experiment to within 5% (see Fig. 1a). The larger differences are concentrated in C II ($\sim$ 8%) and N III ($\sim$ 6%) for the $2s2p^2\ ^4P_J$ and $^2P_{J'}$ levels. Similarly, as shown in Fig. 1b, MVGK give 196 levels for $Z = 8 - 26$ where all agree with experiment to the desirable accuracy. The larger differences are found in O IV for

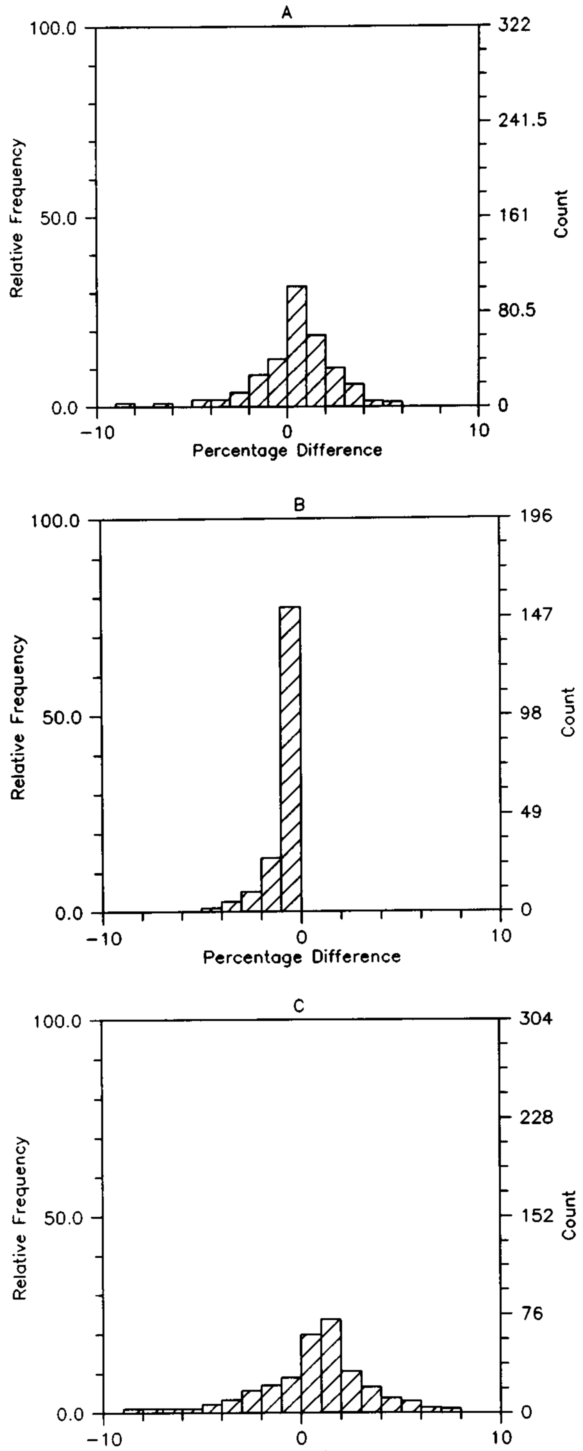

Fig. 1. Histograms showing the percentage difference of the theoretical level energies relative to experiment. **a)** Present dataset, 322 levels for $Z = 6 - 28$. **b)** MVGK, 196 levels for $Z = 8-26$. **c)** CKD, 308 levels for $Z = 7-28$ excluding 4 levels with assignment $2s^2 2p\ ^2P^0_{3/2}$ for $Z < 11$ which show differences greater than 10%

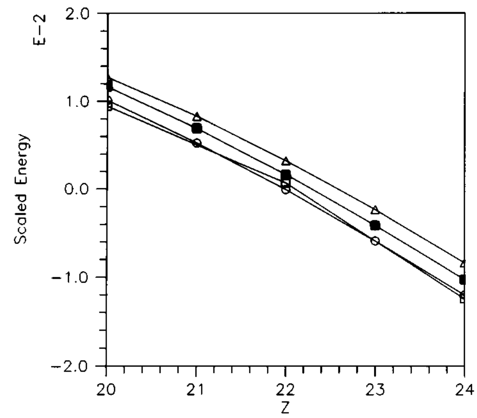

Fig. 2. Energy of the $2s2p^2\ ^2S_{1/2}$ level plotted as a function of Z showing the avoided crossing. For each ion, energies are referred to the center of gravity of the $n = 2$ complex and scaled by its total width. Open circles: experiment. Filled squares: present results. Open squares: MVGK. Open triangles: CKD

the $2p^3\ ^2D^0_J$ and $2s2p^2\ ^2D_{J'}$ levels. Finally, CKD list 308 levels for $Z = 7 - 28$ of which 90% shows a 5% agreement with experiment (see Fig. 1c). The larger discrepancies with experiment are again encountered for the ^4P_J levels ($\sim 9\%$) for $Z \leq 10$ and, more seriously, for the $2s^2 2p\ ^2P^0_{3/2}$ ($Z < 11$) where they reach a factor of 2. Moreover, as depicted in Fig. 1a, in spite of the high accuracy in MVGK all the levels in this dataset are smaller than experiment whereas they should perhaps show the statistical scatter usually found in the ab initio approaches (see Figs. 1a–c).

Among the more interesting features of the B-sequence spectra are a distinctive avoided crossing between the $2s2p^2\ ^2S_{1/2}$ and $^2P_{1/2}$ levels at $Z \sim 22$ and the level switchings that take place within both the $2s2p^2\ ^2D_J$ and $2p^3\ ^2D^0_J$ terms at $Z \sim 14$. In order to depict the avoided crossing, we follow Edlén (1983) by plotting as a function of Z the energy of the $^2S_{1/2}$ level for each ion relative to the center of gravity of the $n = 2$ complex and scaled by its total width (Fig. 2). Taking the change of sign as reference, it can be seen that the experimental crossing takes place just at $Z = 22$. MVGK reproduce this behaviour accurately while the slightly larger energies in the CKD and the present datasets place the crossing at $Z = 23$. It will become clear in the discussions in Sect. 4 that the radiative properties of some transitions near the crossing are severely perturbed; consequently, the intervening interactions should be represented as accurately as possible, but the reliability of such radiative data will generally be very sensitive to small changes. Similarly, in Fig. 3 we show that small discrepancies between the theoretical and experimental level splittings can lead to different predictions of the position of the switching, and in the case of CKD, to an unobserved double switching of the ^2D_J levels.

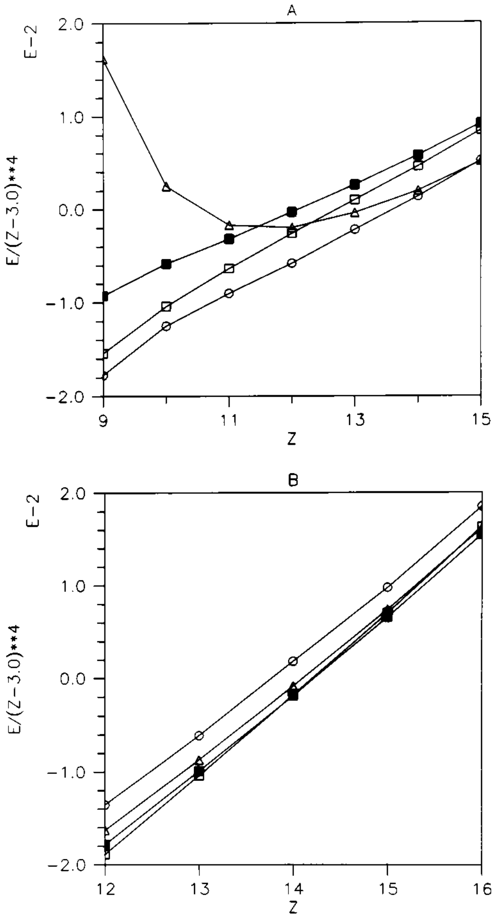

Fig. 3. Scaled energy splitting (Ryd) of the **a)** $2s2p^2\ {}^2D_{3/2}{-}{}^2D_{5/2}$ and **b)** $2p^3\ {}^2D^0_{3/2}{-}{}^2D^0_{5/2}$ levels showing the level switching that takes place at $Z \sim 14$. Open circles: experiment. Filled squares: present results. Open squares: MVGK. Open triangles: CKD. It can be seen that for ${}^2D_J$ CKD predict an unobserved double switching

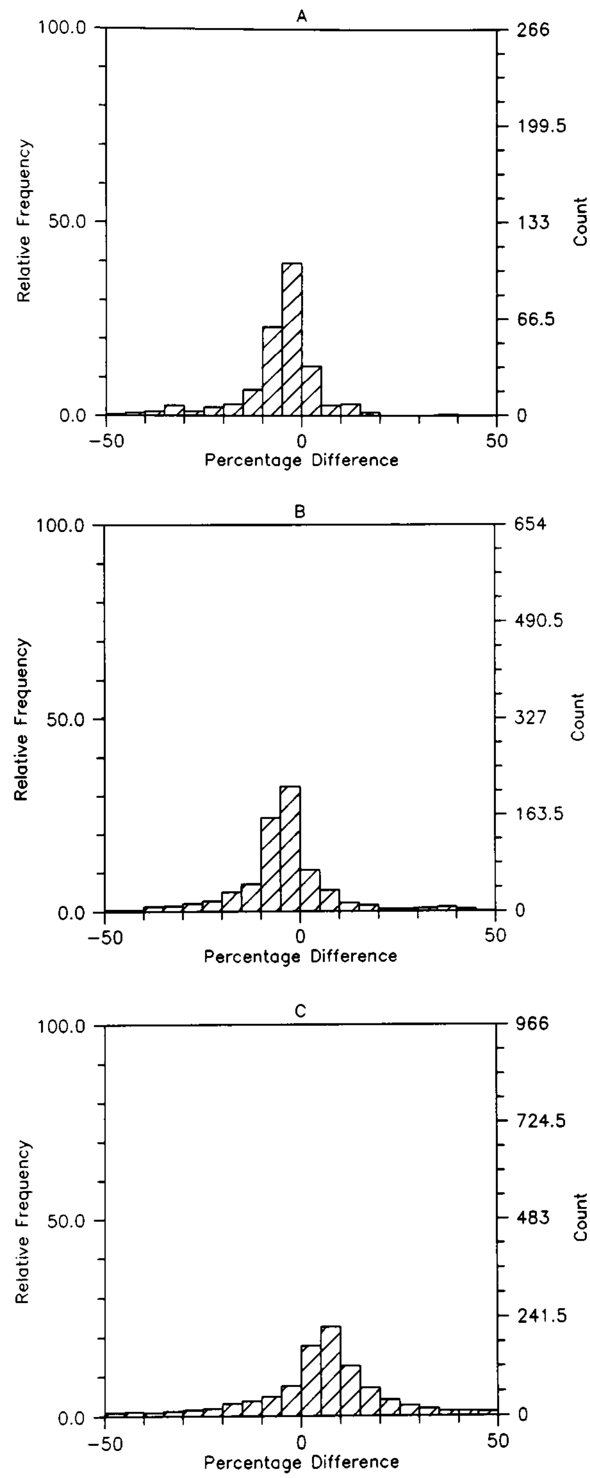

Fig. 4. Histograms showing the percentage difference of the previously computed transition probability datasets with respect to the present results. **a)** DT, 272 A-values for $Z = 6-26$ (excluding 6 A-values showing differences greater than 50%). **b)** MVGK, 686 A-values for $Z = 8-26$ (excluding 32 A-values). **c)** CKD, 1100 A-values for $Z = 7-28$ (excluding 134 A-values for the same reason). It can be concluded that the CKD dataset is of lower statistical reliability

4. Transition probabilities

In the present work we have calculated all the E1, E2 and M1 transitions within the $n = 2$ complex for $Z = 6-28$; this amounts to 2254 transitions. The E2 and M1 transitions are of less importance than the considerably larger E1s, with the notable exception perhaps of the astrophysically relevant forbidden transitions within the ${}^2P^0_J$ ground term. They are nevertheless listed for database purposes. The computed transition probabilities are listed in Tables 3–25.

Comparing the present A-values with previous datasets (see histograms in Fig. 4), it is found that DT list 272 E1 transitions for $Z = 6-26$ of which 77% agree to the desired accuracy (10%), and 6 transitions show discrepancies larger than 50%; namely, the $2s2p^2\ {}^2S_{1/2}{-}2s^22p\ {}^2P^0_{3/2}$ spin-allowed transitions for $Z = 22$ and $Z = 26$ which are affected by the avoided crossing and are discussed

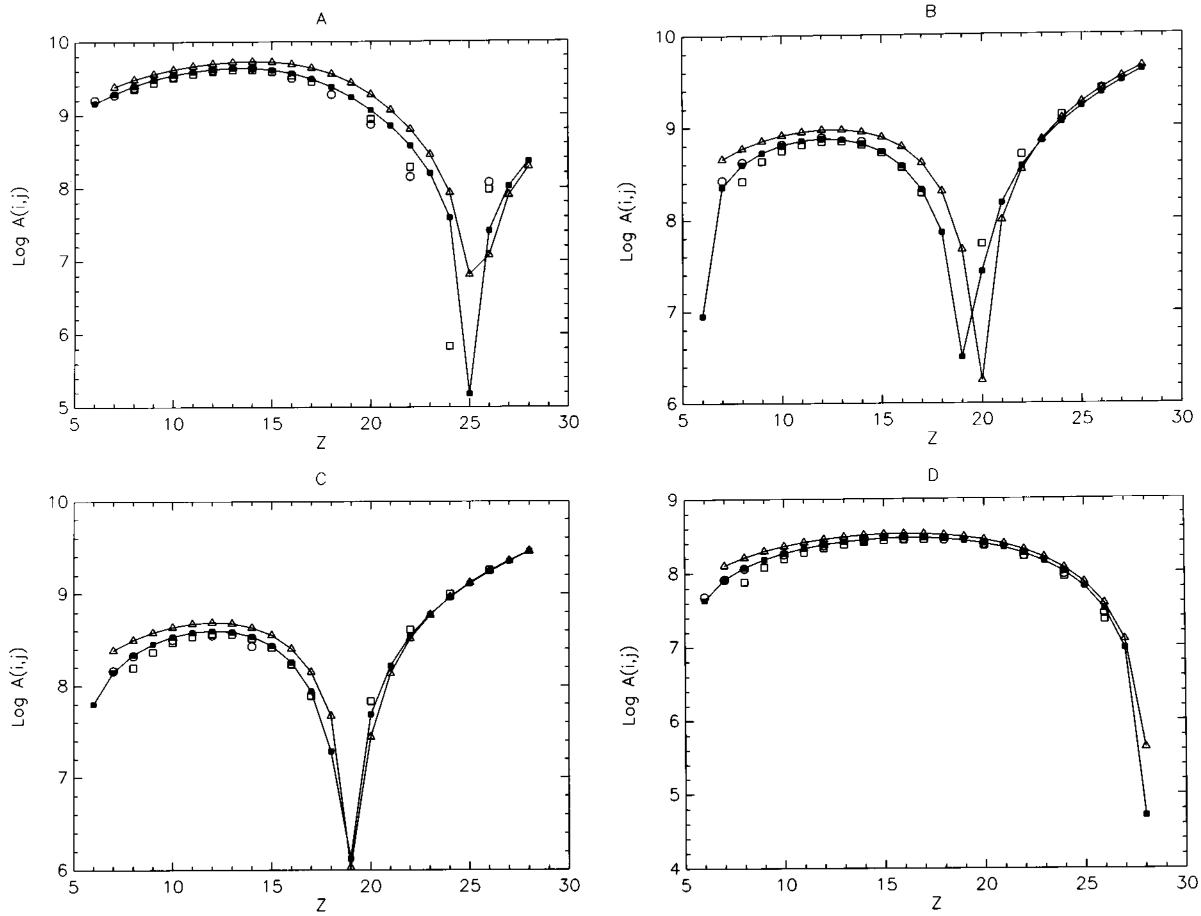

Fig. 5. A-values (s^{-1}) for troublesome spin-allowed transitions as a function of Z. **a)** $2s2p^2\ ^2S_{1/2} - 2s^22p\ ^2P^0_{3/2}$. **b)** $2p^3\ ^2P^0_{1/2} - 2s2p^2\ ^2S_{1/2}$. **c)** $2p^3\ ^2P^0_{1/2} - 2s2p^2\ ^2P_{1/2}$. **d)** $2s2p^2\ ^2D_{3/2} - 2s^22p\ ^2P^0_{3/2}$. Filled squares: present results. Open circles: DT. Open triangles: CKD. Open squares: MVGK

in Sect. 4.1; the $2p^3\ ^2D^0_J$–$2s2p^2\ ^2P_{J'}$ for $Z = 6$ which are perturbed by intermixing $n = 3$ states; and the $2s2p^2\ ^4P_{1/2}$–$2s^22p\ ^2P^0_{3/2}$ intercombination transition for $Z = 6$ (see Sect. 4.2). MVGK list 686 E1 transitions for $Z = 8 - 26$, of which 70% agree with present A-values to 10% and 32 are discrepant by more than 50%; namely, transitions affected by the avoided crossing ($Z > 17$); $2p^3\ ^4S^0_{3/2}$–$2s2p^2\ ^2D_J$ intercombination transitions for $Z < 18$; and transitions for $Z = 8$. The dataset by CKD contains 1100 transitions for $Z = 7 - 28$, mostly E1s but the E2 and M1 transitions within the $^2P^0_J$ ground term are also listed; only 46% agree with the present dataset to within 10% and for 134 transitions the discrepancies are larger than 50%. In general, large discrepancies are found for: the low members of the sequence ($Z < 10$); the transitions affected by the avoided crossing (e.g. $2s2p^2\ ^2S_{1/2}$–$2s^22p\ ^2P^0_{3/2}$, $2p^3\ ^2P^0_{1/2}$–$2s2p^2\ ^2S_{1/2}$ for $Z > 18$); and the intersystem transitions involving the ^4P_J and $^4S^0_{3/2}$ levels for low and intermediate Z. From this comparison it is found that in the range $Z = 7 - 28$, specially for low Z, the CKD dataset differs considerably from the DT, MVGK and present sets.

The present rates allow us to compute radiative lifetimes which can also be compared with recent experiments for C II (Reistad et al. 1986 and Nandi et al. 1996) and N III (Bengtsson et al. 1995). It is found that our theoretical lifetimes lie within the experimental error bars.

We now discuss the problems leading to the larger discrepancies in an attempt to estimate accuracy ratings.

4.1. Spin-allowed E1 transitions

Most of the present transition probabilities for spin-allowed transitions should be accurate to 10%, with the exception of (i) a few transitions for $Z = 6 - 7$ where strong admixture with the low $n = 3$ levels can lead to sensitive A-values and (ii) transitions in highly ionised members of the sequence that are affected by strong relativistic couplings such as those that lead to the avoided crossing of the $2s2p^2\ ^2S_{1/2}$ at $Z \sim 22$. For low Z, this assertion is supported by the

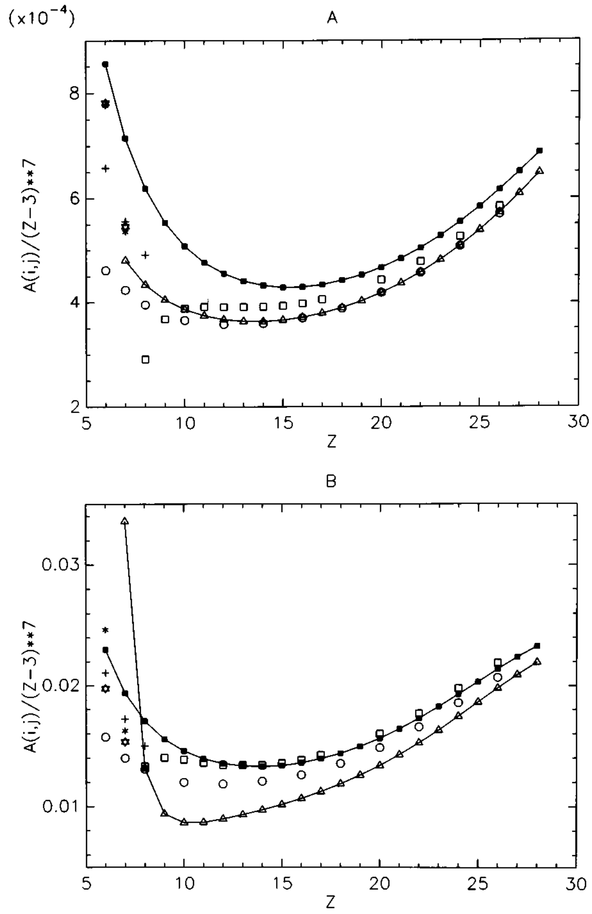

Fig. 6. Scaled A-values (s^{-1}) for the intercombination transitions $2s2p^2\ ^4P_J - 2s^22p\ ^2P^0_{J'}$ as a function of Z showing the large scatter for low Z. **a)** $^4P_{3/2}-^2P^0_{1/2}$. **b)** $^4P_{5/2}-^2P^0_{3/2}$. Filled squares: present results. Open circles: DT. Open triangles: CKD. Open squares: MVGK. Crosses: Froese Fischer (1994), Brage et al. (1995) and Brage et al. (1996). Star: Nussbaumer & Storey (1984, 1979). Asterix: Lennon et al. (1985) and Bell et al. (1995)

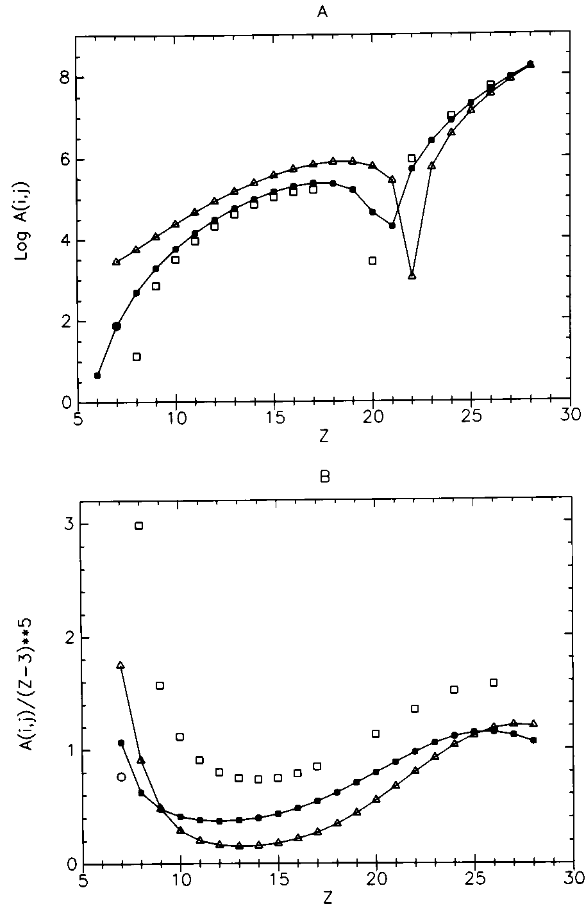

Fig. 7. A-values (s^{-1}) for the intercombination transition $2p^3\ ^2L^0_J-2s2p^2\ ^4P_{J'}$ plotted as a function of Z. **a)** $^2D^0_{3/2}-^4P_{1/2}$ showing the perturbation caused by the avoided crossing at $Z \sim 22$. **b)** $^2P^0_{3/2}-^4P_{1/2}$ showing large differences with MVGK for the whole sequence. Filled squares: present results. Open triangles: CKD. Open squares: MVGK. Open circles: Bell et al (1995)

excellent agreement (∼10%) obtained with the detailed computations by Nussbaumer & Storey (1981), Lennon et al. (1985) and Froese Fischer (1994) on C II; Nussbaumer & Storey (1979), Bell et al. (1995) and Brage et al. (1995) on N III; and Brage et al. (1996) on O IV.

We are therefore not worried, for instance, with the 35% and 40% discrepancies found with DT for the spin-allowed transitions $2p^3\ ^4S^0_{3/2}-2s2p^2\ ^4P_J$ in N III and $2s2p^2\ ^2P_{3/2}-2s^22p\ ^2P^0_{1/2}$ in O IV, respectively. As mentioned before, for high Z a notably problematic transition is $2s2p^2\ ^2S_{1/2}-\ 2s^22p\ ^2P^0_{3/2}$ which, as seen in Fig. 5a, is strongly perturbed by the avoided crossing. Due to the good overall agreement between DT, MVGK and present data, our A-values for $Z < 17$ can be expected to be well within 10%, but for $Z \sim 25$ an accuracy rating would be uncertain. It would have been useful to have A-values for this transition for $Z = 23, 25, 27$ from DT and MVGK, as these would have provided a better picture of the troublesome region. A similar situation is found for the $2p^3\ ^2P^0_{1/2}-2s2p^2\ ^2S_{1/2}$ (Fig. 5b) and $2p^3\ ^2P^0_{1/2}-2s2p^2\ ^2P_{1/2}$ (Fig. 5c) transitions, where the destructive perturbation caused by the avoided crossing leads to poor accuracy ratings for the range $17 < Z < 22$. The accuracy of the A-value at $Z = 6$ for the former transition (see Fig. 5b) is also questionable as it seems to be perturbed by a state belonging to the $n = 3$ configurations. A similar situation is encountered in C II for the transitions $2p^3\ ^2D^0_J-2s2p^2\ ^2P_{J'}$. As shown in Fig. 5d, destructive interference is also found for $Z \sim 28$ in the $2s2p^2\ ^2D_{3/2}-2s^22p\ ^2P^0_{3/2}$ transition, causing the accuracy of the rates for $Z > 26$ to be of lower quality. For most of these difficult transitions (see Figs. 5a–c) the data by CKD are consistently discrepant (differences are greater than 20%) with DT, MVGK and the present dataset throughout the sequence. Also the data by MVGK begin to show significant differences from the present ones for $Z < 12$ where correlation effects are more conspicuous and the

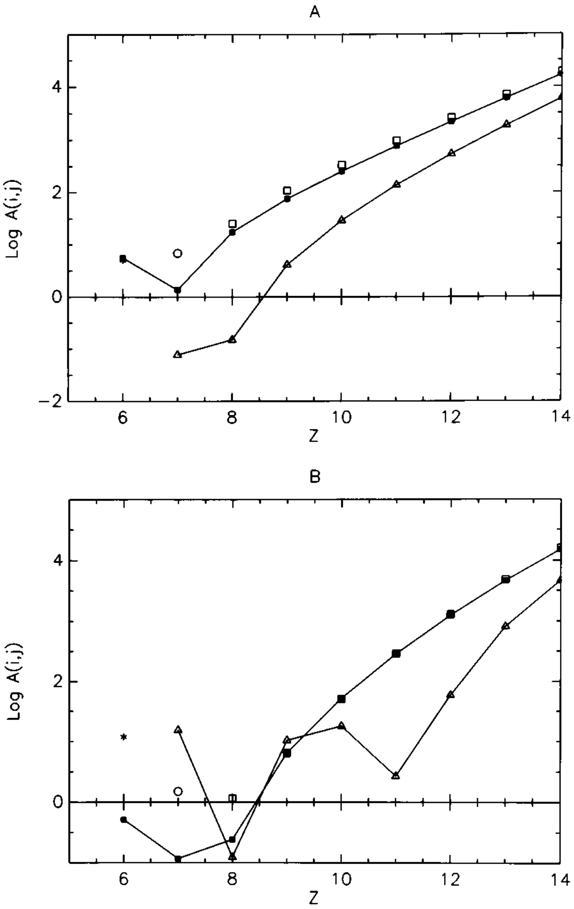

Fig. 8. A-values (s^{-1}) for the $2p^3\ ^4S^0_{3/2} - 2s2p^2\ ^2L_J$ intercombination transitions plotted as a function of Z. **a)** $^4S^0_{3/2} -^2 S_{1/2}$. **b)** $^4S^0_{3/2} -^2 D_{3/2}$. Filled squares: present results. Open triangles: CKD. Open squares: MVGK. Open circles: Bell et al. (1995). Asterix: Nussbaumer & Storey (1981). It may be seen that the agreement for $Z < 9$ is poor and that large discrepancies exist with CKD for even fairly high Z

present CI method is expected to perform with higher reliability.

4.2. Spin-forbidden E1 transitions

In contrast to the good rating assigned to most spin-allowed transitions, the accuracy for the intercombination transitions is noticeably poorer. The typical situation is illustrated in Fig. 6 with the important $2s2p^2\ ^4P_J - 2s^22p\ ^2P^0_{J'}$ transitions. With regard to the DT, CKD, MVGK and present datasets, differences larger than 10% begin to show up for these transitions for $Z < 20$, and for $Z < 10$ the situation becomes critical. In order to assign ratings to this transition array, we compare in Table 26 present rates for $Z = 6 - 8$ with DT, CKD, MVGK, detailed single-system calculations and recent experiments. It may be appreciated that differences between the present data and DT are as large as a factor of 2 for C II and diminish to $\sim 40\%$ for N III and O IV. The situation with respect to CKD is even considerably worse as the differences reach an order of magnitude. Discrepancies with MVGK for O IV are generally small except for $^4P_{3/2} -^2 P^0_{1/2}$ where they reach a factor of 2. A comparison of the present results with the detailed calculations and experiment allows us to assign a realistic 20% rating to the present A-values for $Z = 6 - 8$. Furthermore, a recent measurement of the lifetime of the $^4P_{5/2}$ level in Fe XXII by Hutton et al. (1997) of 14.8±1.0 ns is in excellent agreement with those given by DT (14.2 ns), CKD (14.3 ns), MVGK (13.4 ns) and the present work (13.7 ns). Therefore the 20% rating for these transitions can be safely extended to the whole sequence.

The situation with the $2p^3\ ^2L^0_J - 2s2p^2\ ^4P_{J'}$ transitions is even more serious since, as shown in Fig. 7, the rates can be strongly perturbed by the avoided crossing. Taking into account the good agreement between the present data and those by Bell et al. (1995) for $Z = 7$ we are encouraged to also maintain the 20% rating for such transitions except for $Z = 6$ and around the perturbation ($18 \leq Z \leq 24$). For the intersystem transitions involving the $2p^3\ ^4S^0_{3/2}$, in spite of very large differences found with CKD for $Z < 20$, we find good agreement with MVGK ($\sim 20\%$) for $Z > 12$. However, as shown in Fig. 8, the situation is complicated for $Z < 9$ where very significant differences are encountered with the detailed calculations. For this range we do not attempt a rating assignment.

4.3. Forbidden transitions

The only forbidden transitions that have been previously considered for the B-like ions are the E2 and M1 transitions within the $2s^22p\ ^2P^0_J$ term. In this context present results are in excellent agreement (better than 10%) with those by Froese Fischer (1983). Taking this outcome as a reference, the A-values listed by CKD are found to be highly unreliable for $Z < 12$.

5. Conclusions

We have computed a complete radiative dataset for the $n = 2$ transitions in the astrophysically relevant boron sequence. Extensive comparisons with other calculations and experiment allow us to conclude that the present work is statistically the most reliable to date. This study has been made possible by the facilities in the atomic structure code SUPERSTRUCTURE for the effective rendering of electron correlation effects and relativistic interactions for low to intermediate Z ions as well as for wavefunction optimization. We have also shown that the required degree of accuracy can be attained, even for low-Z ions, with a reduced $n \leq 3$ orbital basis set provided that TECs are used to simulate higher-order effects. Therefore this practical and reliable approach will be extended to generate radiative data for other isoelectronic sequences within the objectives of the IP.

Acknowledgements. Part of the present work was carried out during visits by MEG and CM to the Observatoire de Paris, Meudon, France. The hospitality received is gratefully acknowledged. The visits were funded by the CNRS, IVIC, CONICIT, UNIMET, the Observatoire de Paris and the Ministère des Affaires Étrangères. This research has been supported by CONICIT under contract No. S1-95000521.

References

Bell K.L., Hibbert A., Stafford R.P., Brage T., 1995, MNRAS 272, 909
Bengtsson P., Curtis L.J., Henderson M., et al., 1995, Phys. Scr. 52, 506
Biémont E., Delahaye F., Zeippen C.J., 1994, J. Phys. B 27, 5841
Blum R.D., Pradhan A.K., 1992, ApJS 80, 425
Brage T., Froese Fischer C., Judge P.G., 1995, ApJ 445, 457
Brage T., Judge P.G., Brekke P., 1996, ApJ 464, 1030
Brekke P., Kjeldseth-Moe O., Bartoe J.-D.F., Brueckner G., 1991, ApJS 75, 1337
Carpenter K.G., Robinson R.D., Wahlgren G.M., et al., 1991, ApJ 377, L45
Cheng K.T., Kim Y-K., Desclaux J.P., 1979, At. Data Nucl. Data Tab. 24, 111
Dankwort W., Trefftz E., 1978, A&A 65, 93
Doschek G.A., Feldman U., Van Hoosier M.E., Bartoe J.-D.F., 1976, ApJS 31, 417
Doschek G.A., Feldman U., Cohen L., 1977, ApJS 33, 101
Edlén B., 1983, Phys. Scr. 28, 483
Eissner W., Nussbaumer H., 1969, J. Phys. B 2, 1028
Eissner W., Jones M., Nussbaumer H., 1974, Comput. Phys. Commun. 8, 270
Eissner W., 1991, J. Phys. IV C1, 3
Fang Z., Kwong V.H.S., Wang J., Parkinson W.H., 1993a, Phys. Rev. A 48, 1114
Fang Z., Kwong V.H.S., Parkinson W.H., 1993b, ApJ 413, L141
Froese Fischer C., 1983, J. Phys. B 16, 157
Froese Fischer C., 1994, Phys. Scr. 49, 323
Galavís M.E., Mendoza C., Zeippen C.J., 1997, A&AS 123, 159
Hayes M.A., Nussbaumer H., 1986, A&A 161, 287
Hummer D.G., Berrington K.A., Eissner W., et al., 1993, A&A 279, 298
Hutton R., Martinson I., Nyström B., et al., 1997, Phys. Scr. 55, 431
Jones M., 1970, J. Phys. B 3, 1571
Jones M., 1971, J. Phys. B 4, 1422
Judge P.G., 1986a, MNRAS 221, 119
Judge P.G., 1986b, MNRAS 223, 239
Lennon D.J., Dufton P.L., Hibbert A., Kingston A.E., 1985, ApJ 294, 200
Merkelis G., Vilkas M.J., Gaigalas G., Kisielius R., 1995, Phys. Scr. 51, 233
Moore C.E., 1970, Selected Tables of Atomic Spectra NSRDS-NBS3, US Govt. Printing Office, Washington DC
Moore C.E., 1975, Selected Tables of Atomic Spectra NSRDS-NBS3, US Govt. Printing Office, Washington DC
Nandi T., Bhattacharya N., Kurup M.B., Prasad K.G., 1996, Phys. Scr. 54, 179
Nussbaumer H., Schild H., 1981, A&A 101, 118
Nussbaumer H., Storey P.J., 1978, A&A 64, 139
Nussbaumer H., Storey P.J., 1979, A&A 71, L5
Nussbaumer H., Storey P.J., 1981, A&A 96, 91
Peng J.F., Pradhan A.K., 1995, A&AS 112, 151
Reistad N., Hutton A., Nilsson A.E., Martinson I., 1986, Phys. Scr. 34, 151
Sandlin G.D., Brueckner G.E., Scherrer V.E., Tousey R., 1976, ApJ 205, L47
Stencel R.E., Linsky J.L., Brown A., et al., 1981, MNRAS 196, 47P
Zeippen C.J., Seaton M.J., Morton D.C., 1977, MNRAS 181, 527
Zhang H.L, Graziani M., Pradhan A.K., 1994, A&A 283, 319

Table 3. Transition probabilities (s^{-1}) for C II

j	i	A_{ij}	j	i	A_{ij}	j	i	A_{ij}	j	i	A_{ij}
1	2	2.291E−06	3	4	2.393E−07	5	9	1.575E−06	8	13	9.136E+02
1	3	7.191E+01	3	5	3.657E−14	5	10	3.392E−04	8	14	8.945E+06
1	4	1.871E+00	3	6	5.123E−07	5	11	1.842E+09	8	15	8.365E+06
1	7	2.185E+08	3	7	9.814E−05	5	12	1.292E+03	9	10	6.380E−07
1	8	7.316E+08	3	8	1.212E−03	5	13	1.342E+01	9	11	2.180E+01
1	9	2.779E+09	3	9	5.516E−04	5	15	1.895E+04	9	13	3.326E+07
1	10	6.973E+08	3	10	1.090E−04	6	7	2.529E−10	9	14	2.521E+08
1	11	7.482E−03	3	11	6.150E+08	6	8	2.455E+00	9	15	6.314E+07
1	12	3.399E+03	3	13	4.728E+00	6	9	8.395E−05	10	11	7.494E+01
1	13	7.669E+03	3	14	2.022E+03	6	10	7.499E−04	10	12	3.965E+07
1	14	4.881E−11	3	15	8.286E+03	6	11	2.030E+01	10	13	6.535E+06
1	15	2.627E+03	4	5	3.668E−07	6	12	4.208E+08	10	14	1.256E+08
2	3	8.189E+01	4	6	2.928E−04	6	13	4.585E+07	10	15	3.156E+08
2	4	1.022E+01	4	7	3.659E−04	6	15	1.627E+09	11	12	1.895E−07
2	5	5.031E+01	4	8	6.037E−03	7	8	1.636E+00	11	13	2.281E−06
2	6	2.608E+08	4	9	5.184E−05	7	9	8.300E−04	11	14	4.302E−04
2	7	4.315E+07	4	10	2.560E−04	7	10	1.255E−03	11	15	1.057E−03
2	8	1.444E+09	4	11	1.229E+09	7	11	5.161E−01	12	13	2.147E−09
2	9	1.402E+09	4	12	5.356E+01	7	12	3.015E+07	12	14	2.045E−04
2	10	3.485E+09	4	13	5.096E+02	7	13	4.045E+08	12	15	4.682E−04
2	11	4.719E−03	4	14	5.300E+03	7	14	1.808E+09	13	14	7.574E−04
2	12	1.186E+04	4	15	5.461E+02	7	15	1.814E+08	13	15	6.375E−04
2	13	7.605E+03	5	6	1.331E−03	8	9	6.311E−04	14	15	5.974E−08
2	14	5.259E+03	5	7	1.958E−04	8	10	1.595E−04			
2	15	2.676E+03	5	8	1.320E−05	8	11	5.635E+00			

Table 4. Transition probabilities (s^{-1}) for N III

j	i	A_{ij}	j	i	A_{ij}	j	i	A_{ij}	j	i	A_{ij}
1	2	4.736E−05	3	4	4.783E−06	5	9	8.500E−06	8	13	2.141E+04
1	3	4.177E+02	3	5	2.063E−12	5	10	3.476E−03	8	14	2.251E+08
1	4	1.172E+01	3	6	5.009E−06	5	11	2.625E+09	8	15	2.340E+08
1	7	4.217E+08	3	7	1.055E−03	5	12	1.175E+04	9	10	1.200E−05
1	8	1.001E+09	3	8	1.286E−02	5	13	4.888E+02	9	11	1.155E+02
1	9	3.844E+09	3	9	5.513E−03	5	15	2.815E+03	9	13	1.229E+08
1	10	9.669E+08	3	10	1.095E−03	6	7	4.867E−09	9	14	5.844E+08
1	11	1.566E−02	3	11	8.778E+08	6	8	6.487E+00	9	15	1.412E+08
1	12	2.788E+03	3	13	7.582E+01	6	9	4.678E−02	10	11	4.219E+02
1	13	6.313E+03	3	14	2.621E+03	6	10	1.230E−01	10	12	1.456E+08
1	14	4.441E−13	3	15	1.091E+03	6	11	1.527E+02	10	13	2.385E+07
1	15	3.522E+03	4	5	8.632E−06	6	12	9.583E+08	10	14	2.875E+08
2	3	4.462E+02	4	6	2.792E−03	6	13	1.058E+08	10	15	7.261E+08
2	4	6.996E+01	4	7	3.984E−03	6	15	2.376E+09	11	12	3.085E−06
2	5	3.171E+02	4	8	6.376E−02	7	8	4.314E+00	11	13	2.999E−05
2	6	5.013E+08	4	9	2.955E−04	7	9	1.280E−01	11	14	9.601E−03
2	7	8.239E+07	4	10	2.538E−03	7	10	6.706E−02	11	15	2.398E−02
2	8	1.930E+09	4	11	1.753E+09	7	11	1.168E−01	12	13	4.732E−08
2	9	1.958E+09	4	12	2.362E+02	7	12	6.925E+07	12	14	1.784E+00
2	10	4.838E+09	4	13	3.554E+03	7	13	9.196E+08	12	15	3.138E+00
2	11	1.391E−02	4	14	1.121E+03	7	14	2.655E+09	13	14	2.670E+00
2	12	9.715E+03	4	15	1.256E+04	7	15	2.680E+08	13	15	1.352E+00
2	13	6.212E+03	5	6	1.307E−02	8	9	5.083E−03	14	15	7.148E−10
2	14	7.063E+03	5	7	1.777E−03	8	10	1.301E−03			
2	15	3.623E+03	5	8	2.584E−04	8	11	1.364E+00			

Table 5. Transition probabilities (s^{-1}) for O IV

j	i	A_{ij}	j	i	A_{ij}	j	i	A_{ij}	j	i	A_{ij}
1	2	5.171E−04	3	4	5.053E−05	5	9	4.834E−05	8	13	1.376E+05
1	3	1.724E+03	3	5	4.884E−11	5	10	2.120E−02	8	14	3.927E+08
1	4	4.836E+01	3	6	2.430E−05	5	11	3.396E+09	8	15	4.224E+08
1	7	6.195E+08	3	7	6.622E−03	5	12	5.278E+04	9	10	1.258E−04
1	8	1.340E+09	3	8	7.898E−02	5	13	2.776E+03	9	11	4.547E+02
1	9	4.864E+09	3	9	3.263E−02	5	15	1.341E+04	9	13	2.255E+08
1	10	1.231E+09	3	10	6.679E−03	6	7	4.441E−08	9	14	9.335E+08
1	11	4.750E−02	3	11	1.139E+09	6	8	8.720E+00	9	15	2.172E+08
1	12	2.618E+03	3	13	4.907E+02	6	9	4.514E−02	10	11	1.716E+03
1	13	5.960E+03	3	14	1.288E+04	6	10	1.903E−01	10	12	2.648E+08
1	14	5.328E−12	3	15	1.942E+03	6	11	3.279E+02	10	13	4.282E+07
1	15	4.828E+03	4	5	1.008E−04	6	12	1.447E+09	10	14	4.528E+08
2	3	1.762E+03	4	6	1.650E−02	6	13	1.629E+08	10	15	1.152E+09
2	4	3.147E+02	4	7	2.518E−02	6	15	2.815E+09	11	12	2.131E−05
2	5	1.331E+03	4	8	3.881E−01	7	8	5.786E+00	11	13	2.004E−04
2	6	7.314E+08	4	9	1.065E−03	7	9	2.257E−01	11	14	6.365E−02
2	7	1.189E+08	4	10	1.537E−02	7	10	1.352E−01	11	15	1.588E−01
2	8	2.490E+09	4	11	2.272E+09	7	11	2.394E−01	12	13	3.947E−07
2	9	2.528E+09	4	12	1.068E+03	7	12	1.057E+08	12	14	2.480E+00
2	10	6.169E+09	4	13	1.556E+04	7	13	1.384E+09	12	15	4.389E+00
2	11	5.530E−02	4	14	3.576E+03	7	14	3.158E+09	13	14	3.742E+00
2	12	9.096E+03	4	15	4.452E+04	7	15	3.227E+08	13	15	1.933E+00
2	13	5.785E+03	5	6	7.838E−02	8	9	2.671E−02	14	15	3.084E−09
2	14	9.812E+03	5	7	1.022E−02	8	10	6.989E−03			
2	15	5.033E+03	5	8	1.191E−03	8	11	1.759E+01			

Table 6. Transition probabilities (s^{-1}) for F V

j	i	A_{ij}	j	i	A_{ij}	j	i	A_{ij}	j	i	A_{ij}
1	2	3.718E−03	3	4	3.597E−04	5	9	2.137E−04	8	13	5.833E+05
1	3	5.607E+03	3	5	6.909E−10	5	10	9.377E−02	8	14	5.284E+08
1	4	1.550E+02	3	6	8.466E−05	5	11	4.154E+09	8	15	6.000E+08
1	7	8.168E+08	3	7	3.001E−02	5	12	1.752E+05	9	10	9.389E−04
1	8	1.721E+09	3	8	3.552E−01	5	13	9.861E+03	9	11	1.434E+03
1	9	5.845E+09	3	9	1.397E−01	5	15	4.134E+04	9	13	3.362E+08
1	10	1.494E+09	3	10	2.989E−02	6	7	1.969E−07	9	14	1.299E+09
1	11	1.314E−01	3	11	1.398E+09	6	8	1.061E+01	9	15	2.855E+08
1	12	2.631E+03	3	13	1.948E+03	6	9	1.975E−02	10	11	5.458E+03
1	13	6.038E+03	3	14	4.349E+04	6	10	2.839E−01	10	12	3.899E+08
1	14	6.420E−11	3	15	3.704E+03	6	11	6.927E+02	10	13	6.191E+07
1	15	4.998E+03	4	5	7.805E−04	6	12	1.912E+09	10	14	6.169E+08
2	3	5.506E+03	4	6	7.230E−02	6	13	2.215E+08	10	15	1.586E+09
2	4	1.081E+03	4	7	1.143E−01	6	15	3.414E+09	11	12	1.005E−04
2	5	4.349E+03	4	8	1.721E+00	7	8	7.023E+00	11	13	1.037E−03
2	6	9.553E+08	4	9	3.342E−03	7	9	3.822E−01	11	14	2.948E−01
2	7	1.529E+08	4	10	6.876E−02	7	10	3.062E−01	11	15	7.353E−01
2	8	3.018E+09	4	11	2.785E+09	7	11	6.468E+00	12	13	1.789E−06
2	9	3.135E+09	4	12	3.782E+03	7	12	1.419E+08	12	14	2.965E+00
2	10	7.503E+09	4	13	5.237E+04	7	13	1.820E+09	12	15	5.389E+00
2	11	1.879E−01	4	14	1.064E+04	7	14	3.855E+09	13	14	4.615E+00
2	12	9.110E+03	4	15	1.293E+05	7	15	3.998E+08	13	15	2.553E+00
2	13	5.748E+03	5	6	3.447E−01	8	9	1.061E−01	14	15	5.242E−08
2	14	1.027E+04	5	7	4.397E−02	8	10	2.879E−02			
2	15	5.336E+03	5	8	3.944E−03	8	11	7.625E+01			

Table 7. Transition probabilities in s^{-1} for Ne VI

j	i	A_{ij}	j	i	A_{ij}	j	i	A_{ij}	j	i	A_{ij}
1	2	2.012E−02	3	4	1.967E−03	5	9	7.830E−04	8	13	1.949E+06
1	3	1.544E+04	3	5	6.662E−09	5	10	3.315E−01	8	14	6.354E+08
1	4	4.186E+02	3	6	2.403E−04	5	11	4.908E+09	8	15	7.817E+08
1	7	1.020E+09	3	7	1.087E−01	5	12	4.821E+05	9	10	5.096E−03
1	8	2.164E+09	3	8	1.292E+00	5	13	2.696E+04	9	11	3.896E+03
1	9	6.771E+09	3	9	4.755E−01	5	15	1.078E+05	9	13	4.551E+08
1	10	1.757E+09	3	10	1.076E−01	6	7	4.369E−07	9	14	1.691E+09
1	11	3.341E−01	3	11	1.661E+09	6	8	1.238E+01	9	15	3.422E+08
1	12	2.722E+03	3	13	5.829E+03	6	9	2.982E−04	10	11	1.469E+04
1	13	6.314E+03	3	14	1.197E+05	6	10	5.578E−01	10	12	5.198E+08
1	14	1.475E−12	3	15	6.909E+03	6	11	1.420E+03	10	13	8.048E+07
1	15	5.159E+03	4	5	4.403E−03	6	12	3.372E+09	10	14	7.796E+08
2	3	1.457E+04	4	6	2.570E−01	6	13	2.852E+08	10	15	2.034E+09
2	4	3.078E+03	4	7	4.139E−01	6	15	4.033E+09	11	12	3.869E−04
2	5	1.198E+04	4	8	6.136E+00	7	8	8.168E+00	11	13	4.712E−03
2	6	1.178E+09	4	9	1.277E−02	7	9	7.672E−01	11	14	1.084E+00
2	7	1.845E+08	4	10	2.493E−01	7	10	8.198E−01	11	15	2.699E+00
2	8	3.493E+09	4	11	3.301E+09	7	11	5.227E+01	12	13	5.314E−06
2	9	3.803E+09	4	12	1.106E+04	7	12	1.798E+08	12	14	3.409E+00
2	10	8.852E+09	4	13	1.488E+05	7	13	2.243E+09	12	15	6.668E+00
2	11	5.609E−01	4	14	2.742E+04	7	14	4.594E+09	13	14	5.800E+00
2	12	9.382E+03	4	15	3.250E+05	7	15	4.857E+08	13	15	3.748E+00
2	13	5.856E+03	5	6	1.222E+00	8	9	3.453E−01	14	15	8.189E−07
2	14	1.076E+04	5	7	1.542E−01	8	10	9.881E−02			
2	15	5.689E+03	5	8	1.078E−02	8	11	2.561E+02			

Table 8. Transition probabilities (s^{-1}) for Na VII

j	i	A_{ij}	j	i	A_{ij}	j	i	A_{ij}	j	i	A_{ij}
1	2	8.750E−02	3	4	8.779E−03	5	9	2.518E−03	8	13	5.542E+06
1	3	3.758E+04	3	5	4.857E−08	5	10	9.915E−01	8	14	7.098E+08
1	4	1.000E+03	3	6	5.915E−04	5	11	5.665E+09	8	15	9.775E+08
1	7	1.233E+09	3	7	3.342E−01	5	12	1.164E+06	9	10	2.131E−02
1	8	2.703E+09	3	8	4.024E+00	5	13	6.134E+04	9	11	9.494E+03
1	9	7.620E+09	3	9	1.353E+00	5	15	2.498E+05	9	13	5.826E+08
1	10	2.021E+09	3	10	3.296E−01	6	7	8.196E−07	9	14	2.119E+09
1	11	7.909E−01	3	11	1.930E+09	6	8	1.407E+01	9	15	3.821E+08
1	12	2.855E+03	3	13	1.438E+04	6	9	2.577E−02	10	11	3.499E+04
1	13	6.711E+03	3	14	2.867E+05	6	10	1.328E+00	10	12	6.542E+08
1	14	1.270E−11	3	15	1.249E+04	6	11	2.796E+03	10	13	9.796E+07
1	15	5.324E+03	4	5	1.988E−02	6	12	2.835E+09	10	14	9.402E+08
2	3	3.401E+04	4	6	7.830E−01	6	13	3.572E+08	10	15	2.502E+09
2	4	7.626E+03	4	7	1.267E+00	6	15	4.656E+09	11	12	1.330E−03
2	5	2.918E+04	4	8	1.859E+01	7	8	9.251E+00	11	13	1.965E−02
2	6	1.402E+09	4	9	6.648E−02	7	9	1.719E+00	11	14	3.366E+00
2	7	2.134E+08	4	10	7.742E−01	7	10	2.221E+00	11	15	8.370E+00
2	8	3.891E+09	4	11	3.825E+09	7	11	2.871E+02	12	13	1.028E−05
2	9	4.563E+09	4	12	2.801E+04	7	12	2.208E+08	12	14	3.840E+00
2	10	1.023E+10	4	13	3.750E+05	7	13	2.657E+09	12	15	8.831E+00
2	11	1.503E+00	4	14	6.304E+04	7	14	5.366E+09	13	14	7.942E+00
2	12	9.782E+03	4	15	7.312E+05	7	15	5.811E+08	13	15	6.521E+00
2	13	6.019E+03	5	6	3.689E+00	8	9	9.677E−01	14	15	8.197E−06
2	14	1.132E+04	5	7	4.650E−01	8	10	2.969E−01			
2	15	6.119E+03	5	8	2.574E−02	8	11	7.741E+02			

Table 9. Transition probabilities (s^{-1}) for Mg VIII

j	i	A_{ij}	j	i	A_{ij}	j	i	A_{ij}	j	i	A_{ij}
1	2	3.237E−01	3	4	3.338E−02	5	9	7.365E−03	8	13	1.398E+07
1	3	8.326E+04	3	5	2.848E−07	5	10	2.600E+00	8	14	7.443E+08
1	4	2.180E+03	3	6	1.310E−03	5	11	6.429E+09	8	15	1.196E+09
1	7	1.461E+09	3	7	9.059E−01	5	12	2.546E+06	9	10	7.295E−02
1	8	3.379E+09	3	8	1.115E+01	5	13	1.204E+05	9	11	2.127E+04
1	9	8.358E+09	3	9	3.316E+00	5	15	5.296E+05	9	13	7.188E+08
1	10	2.288E+09	3	10	8.896E−01	6	7	8.877E−07	9	14	2.596E+09
1	11	1.764E+00	3	11	2.209E+09	6	8	1.565E+01	9	15	3.993E+08
1	12	3.016E+03	3	13	3.065E+04	6	9	1.609E−01	10	11	7.578E+04
1	13	7.207E+03	3	14	6.185E+05	6	10	3.258E+00	10	12	7.930E+08
1	14	5.756E−11	3	15	2.196E+04	6	11	5.314E+03	10	13	1.137E+08
1	15	5.476E+03	4	5	7.563E−02	6	12	3.306E+09	10	14	1.098E+09
2	3	7.196E+04	4	6	2.120E+00	6	13	4.409E+08	10	15	2.993E+09
2	4	1.698E+04	4	7	3.413E+00	6	15	5.279E+09	11	12	4.287E−03
2	5	6.470E+04	4	8	4.961E+01	7	8	1.026E+01	11	13	7.605E−02
2	6	1.628E+09	4	9	3.657E−01	7	9	3.906E+00	11	14	9.188E+00
2	7	2.389E+08	4	10	2.135E+00	7	10	5.659E+00	11	15	2.279E+01
2	8	4.183E+09	4	11	4.363E+09	7	11	1.255E+03	12	13	1.139E−05
2	9	5.451E+09	4	12	6.349E+04	7	12	2.664E+08	12	14	4.264E+00
2	10	1.164E+10	4	13	8.653E+05	7	13	3.064E+09	12	15	1.310E+01
2	11	3.678E+00	4	14	1.324E+05	7	14	6.174E+09	13	14	1.235E+01
2	12	1.026E+04	4	15	1.507E+06	7	15	6.883E+08	13	15	1.301E+01
2	13	6.198E+03	5	6	9.839E+00	8	9	2.416E+00	14	15	6.450E−05
2	14	1.194E+04	5	7	1.247E+00	8	10	8.093E−01			
2	15	6.631E+03	5	8	5.539E−02	8	11	2.219E+03			

Table 10. Transition probabilities (s^{-1}) for Al IX

j	i	A_{ij}	j	i	A_{ij}	j	i	A_{ij}	j	i	A_{ij}
1	2	1.051E+00	3	4	1.123E−01	5	9	2.001E−02	8	13	3.213E+07
1	3	1.713E+05	3	5	1.402E−06	5	10	6.130E+00	8	14	7.301E+08
1	4	4.411E+03	3	6	2.220E+00	5	11	7.205E+09	8	15	1.442E+09
1	6	1.709E+09	3	7	2.680E−03	5	12	5.152E+06	9	10	2.135E−01
1	8	4.246E+09	3	8	2.817E+01	5	13	2.073E+05	9	11	4.453E+04
1	9	8.939E+09	3	9	7.119E+00	5	15	1.048E+06	9	13	8.621E+08
1	10	2.557E+09	3	10	2.171E+00	6	7	1.722E−07	9	14	3.133E+09
1	11	3.743E+00	3	11	2.501E+09	6	8	1.118E+01	9	15	3.883E+08
1	12	3.201E+03	3	13	5.784E+04	6	9	8.557E+00	10	11	1.522E+05
1	13	7.800E+03	3	14	1.230E+06	6	10	1.341E+01	10	12	9.364E+08
1	14	5.081E−11	3	15	3.786E+04	6	11	4.637E+03	10	13	1.270E+08
1	15	5.603E+03	4	5	2.498E−01	6	12	3.183E+08	10	14	1.251E+09
2	3	1.406E+05	4	6	8.287E+00	6	13	3.464E+09	10	15	3.516E+09
2	4	3.473E+04	4	7	5.227E+00	6	14	7.023E+09	11	12	1.325E−02
2	5	1.332E+05	4	8	1.195E+02	6	15	8.105E+08	11	13	2.735E−01
2	6	2.605E+08	4	9	1.802E+00	7	8	1.705E+01	11	14	2.266E+01
2	7	1.859E+09	4	10	5.362E+00	7	9	5.101E−01	11	15	5.598E+01
2	8	4.335E+09	4	11	4.919E+09	7	10	7.655E+00	12	13	3.662E−06
2	9	6.508E+09	4	12	1.319E+05	7	11	9.890E+03	12	14	4.682E+00
2	10	1.310E+10	4	13	1.865E+06	7	12	3.791E+09	12	15	2.187E+01
2	11	8.332E+00	4	14	2.581E+05	7	13	5.403E+08	13	14	2.158E+01
2	12	1.080E+04	4	15	2.889E+06	7	15	5.897E+09	13	15	2.749E+01
2	13	6.372E+03	5	6	3.048E+00	8	9	5.501E+00	14	15	4.180E−04
2	14	1.262E+04	5	7	2.376E+01	8	10	2.049E+00			
2	15	7.232E+03	5	8	1.091E−01	8	11	6.156E+03			

Table 11. Transition probabilities (s^{-1}) for Si X

j	i	A_{ij}	j	i	A_{ij}	j	i	A_{ij}	j	i	A_{ij}
1	2	3.071E+00	3	4	3.405E−01	5	9	5.118E−02	8	13	6.822E+07
1	3	3.322E+05	3	5	5.974E−06	5	10	1.322E+01	8	14	6.619E+08
1	4	8.441E+03	3	6	5.021E+00	5	11	7.997E+09	8	15	1.721E+09
1	6	1.981E+09	3	7	5.122E−03	5	12	9.811E+06	9	10	5.426E−01
1	8	5.369E+09	3	8	6.607E+01	5	13	3.146E+05	9	11	8.798E+04
1	9	9.310E+09	3	9	1.345E+01	5	15	1.946E+06	9	13	1.008E+09
1	10	2.830E+09	3	10	4.879E+00	6	7	8.622E−08	9	14	3.740E+09
1	11	7.608E+00	3	11	2.811E+09	6	8	1.203E+01	9	15	3.459E+08
1	12	3.410E+03	3	13	9.788E+04	6	9	1.772E+01	10	11	2.873E+05
1	13	8.501E+03	3	14	2.287E+06	6	10	2.957E+01	10	12	1.085E+09
1	14	2.596E−10	3	15	6.404E+04	6	11	1.519E+04	10	13	1.373E+08
1	15	5.698E+03	4	5	7.366E−01	6	12	3.783E+08	10	14	1.399E+09
2	3	2.572E+05	4	6	1.851E+01	6	13	3.855E+09	10	15	4.077E+09
2	4	6.629E+04	4	7	1.197E+01	6	14	7.924E+09	11	12	3.946E−02
2	5	2.587E+05	4	8	2.638E+02	6	15	9.513E+08	11	13	9.130E−01
2	6	2.773E+08	4	9	7.687E+00	7	8	1.816E+01	11	14	5.145E+01
2	7	2.095E+09	4	10	1.249E+01	7	9	1.227E+00	11	15	1.263E+02
2	8	4.313E+09	4	11	5.499E+09	7	10	1.692E+01	12	13	2.113E−07
2	9	7.775E+09	4	12	2.550E+05	7	11	1.777E+04	12	14	5.096E+00
2	10	1.462E+10	4	13	3.815E+06	7	12	4.293E+09	12	15	3.954E+01
2	11	1.766E+01	4	14	4.747E+05	7	13	6.596E+08	13	14	4.022E+01
2	12	1.140E+04	4	15	5.212E+06	7	15	6.509E+09	13	15	5.792E+01
2	13	6.535E+03	5	6	6.913E+00	8	9	1.163E+01	14	15	2.310E−03
2	14	1.334E+04	5	7	5.297E+01	8	10	4.896E+00			
2	15	7.934E+03	5	8	2.000E−01	8	11	1.661E+04			

Table 12. Transition probabilities (s^{-1}) for P XI

j	i	A_{ij}	j	i	A_{ij}	j	i	A_{ij}	j	i	A_{ij}
1	2	8.213E+00	3	4	9.493E−01	5	9	1.238E−01	8	12	1.351E+08
1	3	6.131E+05	3	5	2.263E−05	5	10	2.640E+01	8	14	5.402E+08
1	4	1.538E+04	3	6	1.060E+01	5	11	8.808E+09	8	15	2.030E+09
1	6	2.284E+09	3	7	9.283E−03	5	12	4.148E+05	9	10	1.212E+00
1	8	6.816E+09	3	8	1.455E+02	5	13	1.774E+07	9	11	1.650E+05
1	9	9.413E+09	3	9	2.230E+01	5	15	3.443E+06	9	12	1.150E+09
1	10	3.106E+09	3	10	1.023E+01	6	7	1.319E−05	9	14	4.420E+09
1	11	1.490E+01	3	11	3.142E+09	6	8	1.301E+01	9	15	2.735E+08
1	12	9.318E+03	3	12	1.489E+05	6	9	3.464E+01	10	11	5.148E+05
1	13	3.646E+03	3	14	4.022E+06	6	10	6.143E+01	10	12	1.439E+08
1	14	2.156E−10	3	15	1.074E+05	6	11	4.481E+04	10	13	1.238E+09
1	15	5.752E+03	4	5	1.977E+00	6	12	4.237E+09	10	14	1.540E+09
2	3	4.444E+05	4	6	3.854E+01	6	13	4.487E+08	10	15	4.685E+09
2	4	1.194E+05	4	7	2.574E+01	6	14	8.886E+09	11	12	2.832E+00
2	5	4.788E+05	4	8	5.392E+02	6	15	1.115E+09	11	13	1.133E−01
2	6	2.886E+08	4	9	2.860E+01	7	8	1.883E+01	11	14	1.091E+02
2	7	2.339E+09	4	10	2.735E+01	7	9	2.522E+00	11	15	2.656E+02
2	8	4.089E+09	4	11	6.106E+09	7	10	3.528E+01	12	13	8.952E−05
2	9	9.287E+09	4	12	7.475E+06	7	11	3.168E+04	12	14	7.615E+01
2	10	1.621E+10	4	13	4.648E+05	7	12	8.042E+08	12	15	1.186E+02
2	11	3.531E+01	4	14	8.291E+05	7	13	4.815E+09	13	14	5.506E+00
2	12	6.674E+03	4	15	8.927E+06	7	15	7.111E+09	13	15	7.386E+01
2	13	1.205E+04	5	6	1.472E+01	8	9	2.326E+01	14	15	1.131E−02
2	14	1.413E+04	5	7	1.103E+02	8	10	1.119E+01			
2	15	8.753E+03	5	8	3.412E−01	8	11	4.364E+04			

Table 13. Transition probabilities (s^{-1}) for S XII

j	i	A_{ij}	j	i	A_{ij}	j	i	A_{ij}	j	i	A_{ij}
1	2	2.038E+01	3	4	2.470E+00	5	9	2.837E−01	8	12	2.503E+08
1	3	1.087E+06	3	5	7.761E−05	5	10	4.930E+01	8	14	3.798E+08
1	4	2.698E+04	3	6	2.119E+01	5	11	9.641E+09	8	15	2.359E+09
1	6	2.625E+09	3	7	1.608E−02	5	12	4.601E+05	9	10	2.387E+00
1	8	8.639E+09	3	8	3.030E+02	5	13	3.078E+07	9	11	2.943E+05
1	9	9.208E+09	3	9	3.205E+01	5	15	5.814E+06	9	12	1.275E+09
1	10	3.386E+09	3	10	2.025E+01	6	7	2.002E−04	9	14	5.161E+09
1	11	2.827E+01	3	11	3.500E+09	6	8	1.469E+01	9	15	1.808E+08
1	12	1.027E+04	3	12	2.023E+05	6	9	6.394E+01	10	11	8.825E+05
1	13	3.910E+03	3	14	6.743E+06	6	10	1.210E+02	10	12	1.462E+08
1	14	6.339E−11	3	15	1.778E+05	6	11	1.215E+05	10	13	1.397E+09
1	15	5.758E+03	4	5	4.890E+00	6	12	4.605E+09	10	14	1.671E+09
2	3	7.311E+05	4	6	7.558E+01	6	13	5.325E+08	10	15	5.352E+09
2	4	2.047E+05	4	7	5.265E+01	6	14	9.922E+09	11	12	8.169E+00
2	5	8.519E+05	4	8	1.029E+03	6	15	1.305E+09	11	13	3.118E−01
2	6	2.936E+08	4	9	9.364E+01	7	8	1.890E+01	11	14	2.188E+02
2	7	2.590E+09	4	10	5.690E+01	7	9	4.624E+00	11	15	5.255E+02
2	8	3.664E+09	4	11	6.747E+09	7	10	6.981E+01	12	13	1.577E−03
2	9	1.105E+10	4	12	1.414E+07	7	11	5.561E+04	12	14	1.421E+02
2	10	1.790E+10	4	13	8.062E+05	7	12	9.795E+08	12	15	2.346E+02
2	11	6.715E+01	4	14	1.388E+06	7	13	5.362E+09	13	14	5.909E+00
2	12	6.788E+03	4	15	1.460E+07	7	15	7.702E+09	13	15	1.378E+02
2	13	1.276E+04	5	6	2.970E+01	8	9	4.466E+01	14	15	4.951E−02
2	14	1.499E+04	5	7	2.172E+02	8	10	2.460E+01			
2	15	9.706E+03	5	8	5.452E−01	8	11	1.108E+05			

Table 14. Transition probabilities (s^{-1}) for Cl XIII

j	i	A_{ij}	j	i	A_{ij}	j	i	A_{ij}	j	i	A_{ij}
1	2	4.744E+01	3	4	6.066E+00	5	9	6.144E−01	8	12	4.335E+08
1	3	1.861E+06	3	5	2.448E−04	5	10	8.663E+01	8	14	2.102E+08
1	4	4.578E+04	3	6	4.035E+01	5	11	1.050E+10	8	15	2.690E+09
1	6	3.013E+09	3	7	2.680E−02	5	12	3.920E+05	9	10	4.145E+00
1	8	1.085E+10	3	8	5.991E+02	5	13	5.151E+07	9	11	5.000E+05
1	9	8.700E+09	3	9	3.906E+01	5	15	9.421E+06	9	12	1.368E+09
1	10	3.669E+09	3	10	3.811E+01	6	7	1.627E−03	9	14	5.937E+09
1	11	5.217E+01	3	11	3.889E+09	6	8	1.848E+01	9	15	8.732E+07
1	12	1.137E+04	3	12	2.396E+05	6	9	1.120E+02	10	11	1.454E+06
1	13	4.206E+03	3	14	1.085E+07	6	10	2.279E+02	10	12	1.440E+08
1	14	6.310E−10	3	15	2.905E+05	6	11	3.066E+05	10	13	1.562E+09
1	15	5.712E+03	4	5	1.128E+01	6	12	4.958E+09	10	14	1.792E+09
2	3	1.151E+06	4	6	1.407E+02	6	13	6.329E+08	10	15	6.089E+09
2	4	3.366E+05	4	7	1.032E+02	6	14	1.104E+10	11	12	2.199E+01
2	5	1.466E+06	4	8	1.840E+03	6	15	1.527E+09	11	13	8.225E−01
2	6	2.919E+08	4	9	2.717E+02	7	8	1.822E+01	11	14	4.180E+02
2	7	2.851E+09	4	10	1.133E+02	7	9	7.740E+00	11	15	9.862E+02
2	8	3.074E+09	4	11	7.425E+09	7	10	1.319E+02	12	13	1.279E−02
2	9	1.304E+10	4	12	2.597E+07	7	11	9.709E+04	12	14	2.577E+02
2	10	1.969E+10	4	13	1.340E+06	7	12	1.191E+09	12	15	4.478E+02
2	11	1.220E+02	4	14	2.241E+06	7	13	5.937E+09	13	14	6.305E+00
2	12	6.879E+03	4	15	2.289E+07	7	15	8.279E+09	13	15	2.523E+02
2	13	1.354E+04	5	6	5.722E+01	8	9	8.377E+01	14	15	1.960E−01
2	14	1.592E+04	5	7	4.072E+02	8	10	5.228E+01			
2	15	1.081E+04	5	8	8.158E−01	8	11	2.703E+05			

Table 15. Transition probabilities (s^{-1}) for Ar XIV

j	i	A_{ij}	j	i	A_{ij}	j	i	A_{ij}	j	i	A_{ij}
1	2	1.045E+02	3	4	1.417E+01	5	9	1.256E+00	8	12	7.024E+08
1	3	3.094E+06	3	5	7.171E−04	5	10	1.439E+02	8	14	7.196E+07
1	4	7.566E+04	3	6	7.373E+01	5	11	1.139E+10	8	15	2.996E+09
1	6	3.456E+09	3	7	4.323E−02	5	12	1.936E+05	9	10	6.348E+00
1	8	1.339E+10	3	8	1.128E+03	5	13	8.363E+07	9	11	8.111E+05
1	9	7.949E+09	3	9	3.885E+01	5	15	1.467E+07	9	12	1.420E+09
1	10	3.956E+09	3	10	6.866E+01	6	7	9.486E−03	9	14	6.713E+09
1	11	9.398E+01	3	11	4.316E+09	6	8	2.704E+01	9	15	1.926E+07
1	12	1.264E+04	3	12	2.345E+05	6	9	1.875E+02	10	11	2.314E+06
1	13	4.538E+03	3	14	1.682E+07	6	10	4.129E+02	10	12	1.374E+08
1	14	3.915E−10	3	15	4.659E+05	6	11	7.276E+05	10	13	1.733E+09
1	15	5.616E+03	4	5	2.448E+01	6	12	5.293E+09	10	14	1.901E+09
2	3	1.742E+06	4	6	2.504E+02	6	13	7.541E+08	10	15	6.909E+09
2	4	5.336E+05	4	7	1.951E+02	6	14	1.227E+10	11	12	5.535E+01
2	5	2.454E+06	4	8	3.102E+03	6	15	1.783E+09	11	13	2.079E+00
2	6	2.830E+08	4	9	7.042E+02	7	8	1.676E+01	11	14	7.667E+02
2	7	3.124E+09	4	10	2.175E+02	7	9	1.199E+01	11	15	1.766E+03
2	8	2.398E+09	4	11	8.145E+09	7	10	2.396E+02	12	13	7.132E−02
2	9	1.520E+10	4	12	4.648E+07	7	11	1.688E+05	12	14	4.514E+02
2	10	2.160E+10	4	13	2.148E+06	7	12	1.444E+09	12	15	8.294E+02
2	11	2.128E+02	4	14	3.503E+06	7	13	6.543E+09	13	14	6.694E+00
2	12	6.959E+03	4	15	3.454E+07	7	15	8.841E+09	13	15	4.500E+02
2	13	1.440E+04	5	6	1.059E+02	8	9	1.561E+02	14	15	7.077E−01
2	14	1.697E+04	5	7	7.323E+02	8	10	1.078E+02			
2	15	1.209E+04	5	8	1.146E+00	8	11	6.292E+05			

Table 16. Transition probabilities (s^{-1}) for K XV

j	i	A_{ij}	j	i	A_{ij}	j	i	A_{ij}	j	i	A_{ij}
1	2	2.194E+02	3	4	3.166E+01	5	9	2.423E+00	8	12	1.067E+09
1	3	5.013E+06	3	5	1.971E−03	5	10	2.268E+02	8	14	3.210E+06
1	4	1.216E+05	3	6	1.299E+02	5	11	1.231E+10	8	15	3.258E+09
1	6	3.967E+09	3	7	6.781E−02	5	12	3.339E+03	9	10	8.623E+00
1	8	1.618E+10	3	8	2.029E+03	5	13	1.321E+08	9	11	1.262E+06
1	9	7.069E+09	3	9	2.920E+01	5	15	2.202E+07	9	12	1.425E+09
1	10	4.246E+09	3	10	1.190E+02	6	7	4.487E−02	9	14	7.451E+09
1	11	1.658E+02	3	11	4.788E+09	6	8	4.424E+01	9	15	1.322E+06
1	12	1.410E+04	3	12	1.633E+05	6	9	3.024E+02	10	11	3.563E+06
1	13	4.913E+03	3	14	2.524E+07	6	10	7.231E+02	10	12	1.270E+08
1	14	4.033E−10	3	15	7.339E+05	6	11	1.634E+06	10	13	1.910E+09
1	15	5.475E+03	4	5	5.030E+01	6	12	5.609E+09	10	14	1.995E+09
2	3	2.540E+06	4	6	4.275E+02	6	13	9.012E+08	10	15	7.829E+09
2	4	8.183E+05	4	7	3.576E+02	6	14	1.361E+10	11	12	1.307E+02
2	5	4.003E+06	4	8	4.964E+03	6	15	2.077E+09	11	13	5.042E+00
2	6	2.667E+08	4	9	1.641E+03	7	8	1.463E+01	11	14	1.359E+03
2	7	3.411E+09	4	10	4.042E+02	7	9	1.736E+01	11	15	3.030E+03
2	8	1.731E+09	4	11	8.910E+09	7	10	4.197E+02	12	13	3.144E−01
2	9	1.743E+10	4	12	8.119E+07	7	11	2.958E+05	12	14	7.627E+02
2	10	2.365E+10	4	13	3.335E+06	7	12	1.742E+09	12	15	1.496E+03
2	11	3.575E+02	4	14	5.319E+06	7	13	7.183E+09	13	14	7.074E+00
2	12	7.052E+03	4	15	5.030E+07	7	15	9.392E+09	13	15	7.810E+02
2	13	1.535E+04	5	6	1.888E+02	8	9	2.922E+02	14	15	2.346E+00
2	14	1.817E+04	5	7	1.268E+03	8	10	2.163E+02			
2	15	1.355E+04	5	8	1.517E+00	8	11	1.395E+06			

Table 17. Transition probabilities (s^{-1}) for Ca XVI

j	i	A_{ij}	j	i	A_{ij}	j	i	A_{ij}	j	i	A_{ij}
1	2	4.412E+02	3	4	6.813E+01	5	9	4.437E+00	8	12	1.531E+09
1	3	7.940E+06	3	5	5.118E−03	5	10	3.393E+02	8	14	2.702E+07
1	4	1.917E+05	3	6	2.221E+02	5	11	1.326E+10	8	15	3.463E+09
1	6	4.559E+09	3	7	1.038E−01	5	12	3.488E+05	9	10	1.050E+01
1	8	1.908E+10	3	8	3.501E+03	5	13	2.040E+08	9	11	1.894E+06
1	9	6.180E+09	3	9	1.330E+01	5	15	3.182E+07	9	12	1.389E+09
1	10	4.538E+09	3	10	1.991E+02	6	7	1.817E−01	9	14	8.132E+09
1	11	2.870E+02	3	11	5.314E+09	6	8	7.440E+01	9	15	4.859E+07
1	12	1.576E+04	3	12	4.468E+04	6	9	4.750E+02	10	11	5.321E+06
1	13	5.338E+03	3	14	3.678E+07	6	10	1.230E+03	10	12	1.138E+08
1	14	2.020E−09	3	15	1.123E+06	6	11	3.497E+06	10	13	2.093E+09
1	15	5.297E+03	4	5	9.836E+01	6	12	5.905E+09	10	14	2.073E+09
2	3	3.581E+06	4	6	7.039E+02	6	13	1.080E+09	10	15	8.867E+09
2	4	1.220E+06	4	7	6.383E+02	6	14	1.509E+10	11	12	2.908E+02
2	5	6.393E+06	4	8	7.603E+03	6	15	2.409E+09	11	13	1.176E+01
2	6	2.434E+08	4	9	3.484E+03	7	8	1.209E+01	11	14	2.338E+03
2	7	3.713E+09	4	10	7.299E+02	7	9	2.379E+01	11	15	4.999E+03
2	8	1.153E+09	4	11	9.720E+09	7	10	7.122E+02	12	13	1.159E+00
2	9	1.969E+10	4	12	1.388E+08	7	11	5.186E+05	12	14	1.244E+03
2	10	2.587E+10	4	13	5.033E+06	7	12	2.087E+09	12	15	2.644E+03
2	11	5.801E+02	4	14	7.877E+06	7	13	7.858E+09	13	14	7.445E+00
2	12	7.192E+03	4	15	7.084E+07	7	15	9.935E+09	13	15	1.321E+03
2	13	1.642E+04	5	6	3.257E+02	8	9	5.510E+02	14	15	7.181E+00
2	14	1.955E+04	5	7	2.129E+03	8	10	4.231E+02			
2	15	1.523E+04	5	8	1.908E+00	8	11	2.952E+06			

Table 18. Transition probabilities (s^{-1}) for Sc XVII

j	i	A_{ij}	j	i	A_{ij}	j	i	A_{ij}	j	i	A_{ij}
1	2	8.543E+02	3	4	1.418E+02	5	9	7.770E+00	8	12	2.092E+09
1	3	1.232E+07	3	5	1.265E−02	5	10	4.820E+02	8	14	1.502E+08
1	4	2.966E+05	3	6	3.694E+02	5	11	1.425E+10	8	15	3.612E+09
1	6	5.246E+09	3	7	1.555E−01	5	12	2.522E+06	9	10	1.163E+01
1	8	2.205E+10	3	8	5.833E+03	5	13	3.084E+08	9	11	2.761E+06
1	9	5.359E+09	3	9	7.965E−01	5	15	4.428E+07	9	12	1.321E+09
1	10	4.832E+09	3	10	3.229E+02	6	7	6.532E−01	9	14	8.753E+09
1	11	4.888E+02	3	11	5.903E+09	6	8	1.214E+02	9	15	1.653E+08
1	12	1.766E+04	3	12	2.050E+04	6	9	7.325E+02	10	11	7.711E+06
1	13	5.820E+03	3	14	5.213E+07	6	10	2.039E+03	10	12	9.936E+07
1	14	3.155E−09	3	15	1.667E+06	6	11	7.159E+06	10	13	2.281E+09
1	15	5.097E+03	4	5	1.838E+02	6	12	6.186E+09	10	14	2.133E+09
2	3	4.886E+06	4	6	1.121E+03	6	13	1.299E+09	10	15	1.004E+10
2	4	1.771E+06	4	7	1.113E+03	6	14	1.674E+10	11	12	6.103E+02
2	5	1.001E+07	4	8	1.123E+04	6	15	2.776E+09	11	13	2.647E+01
2	6	2.137E+08	4	9	6.836E+03	7	8	9.450E+00	11	14	3.923E+03
2	7	4.034E+09	4	10	1.285E+03	7	9	3.129E+01	11	15	7.955E+03
2	8	6.999E+08	4	11	1.058E+10	7	10	1.174E+03	12	13	3.705E+00
2	9	2.195E+10	4	12	2.321E+08	7	11	9.117E+05	12	14	1.960E+03
2	10	2.829E+10	4	13	7.408E+06	7	12	2.476E+09	12	15	4.594E+03
2	11	9.104E+02	4	14	1.141E+07	7	13	8.571E+09	13	14	7.806E+00
2	12	7.444E+03	4	15	9.668E+07	7	15	1.048E+10	13	15	2.179E+03
2	13	1.763E+04	5	6	5.444E+02	8	9	1.038E+03	14	15	2.038E+01
2	14	2.120E+04	5	7	3.473E+03	8	10	8.066E+02			
2	15	1.712E+04	5	8	2.298E+00	8	11	5.988E+06			

Table 19. Transition probabilities (s^{-1}) for Ti XVIII

j	i	A_{ij}	j	i	A_{ij}	j	i	A_{ij}	j	i	A_{ij}
1	2	1.599E+03	3	4	2.864E+02	5	9	1.314E+01	8	12	2.750E+09
1	3	1.875E+07	3	5	2.988E−02	5	10	6.493E+02	8	14	3.740E+08
1	4	4.514E+05	3	6	6.003E+02	5	11	1.528E+10	8	15	3.708E+09
1	6	6.047E+09	3	7	2.278E−01	5	12	9.168E+06	9	10	1.192E+01
1	8	2.509E+10	3	8	9.439E+03	5	13	4.576E+08	9	11	3.917E+06
1	9	4.624E+09	3	9	8.832E+00	5	15	5.932E+07	9	12	1.230E+09
1	10	5.126E+09	3	10	5.090E+02	6	7	2.138E+00	9	14	9.323E+09
1	11	8.203E+02	3	11	6.565E+09	6	8	1.879E+02	9	15	3.505E+08
1	12	1.981E+04	3	12	5.209E+05	6	9	1.114E+03	10	11	1.085E+07
1	13	6.369E+03	3	14	7.198E+07	6	10	3.315E+03	10	12	8.505E+07
1	14	3.278E−09	3	15	2.406E+06	6	11	1.407E+07	10	13	2.474E+09
1	15	4.891E+03	4	5	3.295E+02	6	12	6.452E+09	10	14	2.174E+09
2	3	6.456E+06	4	6	1.731E+03	6	13	1.565E+09	10	15	1.139E+10
2	4	2.511E+06	4	7	1.903E+03	6	14	1.856E+10	11	12	1.214E+03
2	5	1.539E+07	4	8	1.610E+04	6	15	3.175E+09	11	13	5.762E+01
2	6	1.789E+08	4	9	1.261E+04	7	8	6.987E+00	11	14	6.445E+03
2	7	4.376E+09	4	10	2.211E+03	7	9	3.997E+01	11	15	1.223E+04
2	8	3.710E+08	4	11	1.147E+10	7	10	1.884E+03	12	13	1.049E+01
2	9	2.424E+10	4	12	3.804E+08	7	11	1.604E+06	12	14	2.985E+03
2	10	3.092E+10	4	13	1.067E+07	7	12	2.907E+09	12	15	7.876E+03
2	11	1.384E+03	4	14	1.618E+07	7	13	9.319E+09	13	14	8.156E+00
2	12	7.897E+03	4	15	1.282E+08	7	15	1.105E+10	13	15	3.521E+03
2	13	1.902E+04	5	6	8.831E+02	8	9	1.926E+03	14	15	5.388E+01
2	14	2.317E+04	5	7	5.527E+03	8	10	1.498E+03			
2	15	1.927E+04	5	8	2.667E+00	8	11	1.172E+07			

Table 20. Transition probabilities (s^{-1}) for V XIX

j	i	A_{ij}	j	i	A_{ij}	j	i	A_{ij}	j	i	A_{ij}
1	2	2.903E+03	3	4	5.629E+02	5	9	2.157E+01	8	12	3.500E+09
1	3	2.804E+07	3	5	6.779E−02	5	10	8.262E+02	8	14	6.973E+08
1	4	6.765E+05	3	6	9.557E+02	5	11	1.633E+10	8	15	3.764E+09
1	6	6.981E+09	3	7	3.272E−01	5	12	2.505E+07	9	10	1.155E+01
1	8	2.819E+10	3	8	1.490E+04	5	13	6.674E+08	9	11	5.418E+06
1	9	3.991E+09	3	9	6.371E+01	5	15	7.646E+07	9	12	1.124E+09
1	10	5.419E+09	3	10	7.821E+02	6	7	6.460E+00	9	14	9.858E+09
1	11	1.358E+03	3	11	7.314E+09	6	8	2.743E+02	9	15	6.002E+08
1	12	2.223E+04	3	12	2.546E+06	6	9	1.679E+03	10	11	1.480E+07
1	13	6.997E+03	3	14	9.698E+07	6	10	5.259E+03	10	12	7.230E+07
1	14	8.788E−11	3	15	3.359E+06	6	11	2.657E+07	10	13	2.671E+09
1	15	4.695E+03	4	5	5.678E+02	6	12	6.711E+09	10	14	2.194E+09
2	3	8.265E+06	4	6	2.599E+03	6	13	1.891E+09	10	15	1.292E+10
2	4	3.485E+06	4	7	3.197E+03	6	14	2.060E+10	11	12	2.298E+03
2	5	2.325E+07	4	8	2.252E+04	6	15	3.598E+09	11	13	1.216E+02
2	6	1.407E+08	4	9	2.206E+04	7	8	4.853E+00	11	14	1.040E+04
2	7	4.743E+09	4	10	3.726E+03	7	9	4.987E+01	11	15	1.820E+04
2	8	1.568E+08	4	11	1.239E+10	7	10	2.951E+03	12	13	2.667E+01
2	9	2.660E+10	4	12	6.105E+08	7	11	2.805E+06	12	14	4.395E+03
2	10	3.380E+10	4	13	1.505E+07	7	12	3.371E+09	12	15	1.335E+04
2	11	2.036E+03	4	14	2.252E+07	7	13	1.010E+10	13	14	8.495E+00
2	12	8.683E+03	4	15	1.654E+08	7	15	1.165E+10	13	15	5.583E+03
2	13	2.062E+04	5	6	1.391E+03	8	9	3.493E+03	14	15	1.333E+02
2	14	2.560E+04	5	7	8.609E+03	8	10	2.710E+03			
2	15	2.167E+04	5	8	2.994E+00	8	11	2.220E+07			

Table 21. Transition probabilities (s^{-1}) for Cr XX

j	i	A_{ij}	j	i	A_{ij}	j	i	A_{ij}	j	i	A_{ij}
1	2	5.127E+03	3	4	1.079E+03	5	9	3.458E+01	8	12	4.343E+09
1	3	4.123E+07	3	5	1.482E−01	5	10	9.861E+02	8	14	1.123E+09
1	4	9.998E+05	3	6	1.494E+03	5	11	1.742E+10	8	15	3.788E+09
1	6	8.073E+09	3	7	4.611E−01	5	12	5.796E+07	9	10	1.080E+01
1	8	3.141E+10	3	8	2.306E+04	5	13	9.577E+08	9	11	7.304E+06
1	9	3.450E+09	3	9	2.018E+02	5	15	9.478E+07	9	12	1.013E+09
1	10	5.709E+09	3	10	1.173E+03	6	7	1.821E+01	9	14	1.037E+10
1	11	2.216E+03	3	11	8.163E+09	6	8	3.783E+02	9	15	9.120E+08
1	12	2.493E+04	3	12	8.090E+06	6	9	2.510E+03	10	11	1.955E+07
1	13	7.716E+03	3	14	1.276E+08	6	10	8.231E+03	10	12	6.212E+07
1	14	4.057E−09	3	15	4.529E+06	6	11	4.829E+07	10	13	2.871E+09
1	15	4.526E+03	4	5	9.425E+02	6	12	6.967E+09	10	14	2.192E+09
2	3	1.026E+07	4	6	3.800E+03	6	13	2.288E+09	10	15	1.469E+10
2	4	4.744E+06	4	7	5.286E+03	6	14	2.288E+10	11	12	4.161E+03
2	5	3.453E+07	4	8	3.083E+04	6	15	4.037E+09	11	13	2.495E+02
2	6	1.015E+08	4	9	3.700E+04	7	8	3.132E+00	11	14	1.651E+04
2	7	5.137E+09	4	10	6.162E+03	7	9	6.105E+01	11	15	2.623E+04
2	8	3.901E+07	4	11	1.332E+10	7	10	4.516E+03	12	13	6.147E+01
2	9	2.904E+10	4	12	9.595E+08	7	11	4.848E+06	12	14	6.256E+03
2	10	3.698E+10	4	13	2.088E+07	7	12	3.859E+09	12	15	2.238E+04
2	11	2.903E+03	4	14	3.082E+07	7	13	1.091E+10	13	14	8.821E+00
2	12	9.985E+03	4	15	2.082E+08	7	15	1.231E+10	13	15	8.715E+03
2	13	2.250E+04	5	6	2.133E+03	8	9	6.160E+03	14	15	3.101E+02
2	14	2.862E+04	5	7	1.316E+04	8	10	4.786E+03			
2	15	2.436E+04	5	8	3.259E+00	8	11	4.075E+07			

Table 22. Transition probabilities (s^{-1}) for Mn XXI

j	i	A_{ij}	j	i	A_{ij}	j	i	A_{ij}	j	i	A_{ij}
1	2	8.831E+03	3	4	2.022E+03	5	9	5.426E+01	8	12	5.279E+09
1	3	5.964E+07	3	5	3.131E−01	5	10	1.092E+03	8	14	1.659E+09
1	4	1.458E+06	3	6	2.300E+03	5	11	1.852E+10	8	15	3.792E+09
1	6	9.349E+09	3	7	6.379E−01	5	12	1.194E+08	9	10	1.003E+01
1	8	3.478E+10	3	8	3.508E+04	5	13	1.354E+09	9	11	9.570E+06
1	9	2.986E+09	3	9	4.715E+02	5	15	1.129E+08	9	12	9.008E+08
1	10	5.993E+09	3	10	1.722E+03	6	7	4.825E+01	9	14	1.087E+10
1	11	3.566E+03	3	11	9.126E+09	6	8	4.951E+02	9	15	1.287E+09
1	12	2.793E+04	3	12	2.065E+07	6	9	3.724E+03	10	11	2.495E+07
1	13	8.542E+03	3	14	1.642E+08	6	10	1.271E+04	10	12	5.517E+07
1	14	4.096E−09	3	15	5.884E+06	6	11	8.439E+07	10	13	3.072E+09
1	15	4.397E+03	4	5	1.510E+03	6	12	7.225E+09	10	14	2.169E+09
2	3	1.233E+07	4	6	5.418E+03	6	13	2.773E+09	10	15	1.673E+10
2	4	6.344E+06	4	7	8.612E+03	6	14	2.544E+10	11	12	7.247E+03
2	5	5.042E+07	4	8	4.139E+04	6	15	4.482E+09	11	13	4.983E+02
2	6	6.420E+07	4	9	5.991E+04	7	8	1.842E+00	11	14	2.588E+04
2	7	5.564E+09	4	10	1.001E+04	7	9	7.343E+01	11	15	3.660E+04
2	8	1.519E+05	4	11	1.423E+10	7	10	6.764E+03	12	13	1.293E+02
2	9	3.161E+10	4	12	1.475E+09	7	11	8.196E+06	12	14	8.602E+03
2	10	4.048E+10	4	13	2.852E+07	7	12	4.365E+09	12	15	3.716E+04
2	11	4.004E+03	4	14	4.148E+07	7	13	1.174E+10	13	14	9.136E+00
2	12	1.206E+04	4	15	2.562E+08	7	15	1.305E+10	13	15	1.341E+04
2	13	2.471E+04	5	6	3.180E+03	8	9	1.054E+04	14	15	6.813E+02
2	14	3.242E+04	5	7	1.980E+04	8	10	8.263E+03			
2	15	2.739E+04	5	8	3.435E+00	8	11	7.244E+07			

Table 23. Transition probabilities (s^{-1}) for Fe XXII

j	i	A_{ij}	j	i	A_{ij}	j	i	A_{ij}	j	i	A_{ij}
1	2	1.486E+04	3	4	3.708E+03	5	9	8.360E+01	8	12	6.308E+09
1	3	8.495E+07	3	5	6.410E−01	5	10	1.001E+03	8	14	2.319E+09
1	4	2.099E+06	3	6	3.493E+03	5	11	1.962E+10	8	15	3.783E+09
1	6	1.084E+10	3	7	8.663E−01	5	12	2.249E+08	9	10	9.466E+00
1	8	3.835E+10	3	8	5.261E+04	5	13	1.885E+09	9	11	1.213E+07
1	9	2.584E+09	3	9	9.347E+02	5	15	1.291E+08	9	12	7.925E+08
1	10	6.267E+09	3	10	2.475E+03	6	7	1.208E+02	9	14	1.138E+10
1	11	5.653E+03	3	11	1.022E+10	6	8	6.175E+02	9	15	1.728E+09
1	12	3.121E+04	3	12	4.569E+07	6	9	5.490E+03	10	11	3.066E+07
1	13	9.494E+03	3	14	2.067E+08	6	10	1.940E+04	10	12	5.176E+07
1	14	4.163E−09	3	15	7.365E+06	6	11	1.416E+08	10	13	3.273E+09
1	15	4.318E+03	4	5	2.335E+03	6	12	7.489E+09	10	14	2.125E+09
2	3	1.436E+07	4	6	7.543E+03	6	13	3.364E+09	10	15	1.910E+10
2	4	8.345E+06	4	7	1.385E+04	6	14	2.831E+10	11	12	1.222E+04
2	5	7.233E+07	4	8	5.460E+04	6	15	4.922E+09	11	13	9.692E+02
2	6	3.220E+07	4	9	9.415E+04	7	8	9.592E−01	11	14	4.004E+04
2	7	6.028E+09	4	10	1.601E+04	7	9	8.683E+01	11	15	4.949E+04
2	8	2.603E+07	4	11	1.508E+10	7	10	9.924E+03	12	13	2.496E+02
2	9	3.433E+10	4	12	2.217E+09	7	11	1.341E+07	12	14	1.140E+04
2	10	4.436E+10	4	13	3.844E+07	7	12	4.879E+09	12	15	6.097E+04
2	11	5.340E+03	4	14	5.499E+07	7	13	1.258E+10	13	14	9.438E+00
2	12	1.528E+04	4	15	3.087E+08	7	15	1.391E+10	13	15	2.040E+04
2	13	2.735E+04	5	6	4.615E+03	8	9	1.751E+04	14	15	1.420E+03
2	14	3.724E+04	5	7	2.939E+04	8	10	1.395E+04			
2	15	3.080E+04	5	8	3.506E+00	8	11	1.244E+08			

Table 24. Transition probabilities (s^{-1}) for Co XXIII

j	i	A_{ij}	j	i	A_{ij}	j	i	A_{ij}	j	i	A_{ij}
1	2	2.450E+04	3	4	6.664E+03	5	9	1.267E+02	8	12	7.434E+09
1	3	1.191E+08	3	5	1.275E+00	5	10	9.737E+02	8	14	3.119E+09
1	4	2.986E+06	3	6	5.241E+03	5	11	2.070E+10	8	15	3.768E+09
1	6	1.258E+10	3	7	1.154E+00	5	12	3.920E+08	9	10	9.199E+00
1	8	4.219E+10	3	8	7.793E+04	5	13	2.588E+09	9	11	1.478E+07
1	9	2.236E+09	3	9	1.664E+03	5	15	1.417E+08	9	12	6.910E+08
1	10	6.531E+09	3	10	3.489E+03	6	7	2.875E+02	9	14	1.189E+10
1	11	8.803E+03	3	11	1.146E+10	6	8	7.369E+02	9	15	2.244E+09
1	12	3.475E+04	3	12	9.064E+07	6	9	8.037E+03	10	11	3.616E+07
1	13	1.059E+04	3	14	2.548E+08	6	10	2.929E+04	10	12	5.204E+07
1	14	3.826E−09	3	15	8.884E+06	6	11	2.278E+08	10	13	3.472E+09
1	15	4.292E+03	4	5	3.494E+03	6	12	7.761E+09	10	14	2.060E+09
2	3	1.617E+07	4	6	1.027E+04	6	13	4.084E+09	10	15	2.184E+10
2	4	1.081E+07	4	7	2.200E+04	6	14	3.156E+10	11	12	2.011E+04
2	5	1.019E+08	4	8	7.088E+04	6	15	5.349E+09	11	13	1.837E+03
2	6	9.440E+06	4	9	1.442E+05	7	8	4.218E−01	11	14	6.123E+04
2	7	6.535E+09	4	10	2.522E+04	7	9	1.010E+02	11	15	6.479E+04
2	8	1.053E+08	4	11	1.584E+10	7	10	1.426E+04	12	13	4.441E+02
2	9	3.726E+10	4	12	3.250E+09	7	11	2.099E+07	12	14	1.455E+04
2	10	4.868E+10	4	13	5.119E+07	7	12	5.398E+09	12	15	9.871E+04
2	11	6.882E+03	4	14	7.187E+07	7	13	1.342E+10	13	14	9.727E+00
2	12	2.013E+04	4	15	3.650E+08	7	15	1.490E+10	13	15	3.070E+04
2	13	3.054E+04	5	6	6.520E+03	8	9	2.828E+04	14	15	2.824E+03
2	14	4.340E+04	5	7	4.313E+04	8	10	2.306E+04			
2	15	3.466E+04	5	8	3.462E+00	8	11	2.056E+08			

Table 25. Transition probabilities (s^{-1}) for Ni XXIV

j	i	A_{ij}	j	i	A_{ij}	j	i	A_{ij}	j	i	A_{ij}
1	2	3.963E+04	3	4	1.175E+04	5	9	1.894E+02	8	12	8.665E+09
1	3	1.645E+08	3	5	2.466E+00	5	10	7.051E+02	8	14	4.080E+09
1	4	4.199E+06	3	6	7.786E+03	5	11	2.174E+10	8	15	3.752E+09
1	6	1.462E+10	3	7	1.507E+00	5	12	6.381E+08	9	10	9.288E+00
1	8	4.636E+10	3	8	1.142E+05	5	13	3.502E+09	9	11	1.722E+07
1	9	1.933E+09	3	9	2.745E+03	5	15	1.491E+08	9	12	5.981E+08
1	10	6.780E+09	3	10	4.828E+03	6	7	6.519E+02	9	14	1.242E+10
1	11	1.344E+04	3	11	1.286E+10	6	8	8.445E+02	9	15	2.845E+09
1	12	3.852E+04	3	12	1.641E+08	6	9	1.169E+04	10	11	4.078E+07
1	13	1.186E+04	3	14	3.076E+08	6	10	4.382E+04	10	12	5.615E+07
1	14	3.861E−09	3	15	1.034E+07	6	11	3.503E+08	10	13	3.667E+09
1	15	4.324E+03	4	5	5.057E+03	6	12	8.043E+09	10	14	1.977E+09
2	3	1.760E+07	4	6	1.368E+04	6	13	4.957E+09	10	15	2.503E+10
2	4	1.381E+07	4	7	3.451E+04	6	14	3.522E+10	11	12	3.251E+04
2	5	1.409E+08	4	8	9.065E+04	6	15	5.757E+09	11	13	3.390E+03
2	6	5.113E+04	4	9	2.159E+05	7	8	1.441E−01	11	14	9.253E+04
2	7	7.093E+09	4	10	3.914E+04	7	9	1.156E+02	11	15	8.218E+04
2	8	2.291E+08	4	11	1.646E+10	7	10	2.006E+04	12	13	7.308E+02
2	9	4.042E+10	4	12	4.641E+09	7	11	3.110E+07	12	14	1.787E+04
2	10	5.350E+10	4	13	6.742E+07	7	12	5.921E+09	12	15	1.574E+05
2	11	8.570E+03	4	14	9.271E+07	7	13	1.425E+10	13	14	1.000E+01
2	12	2.722E+04	4	15	4.241E+08	7	15	1.606E+10	13	15	4.578E+04
2	13	3.439E+04	5	6	8.973E+03	8	9	4.455E+04	14	15	5.379E+03
2	14	5.129E+04	5	7	6.275E+04	8	10	3.736E+04			
2	15	3.904E+04	5	8	3.305E+00	8	11	3.255E+08			

Table 26. Comparison of present A-values (s^{-1}) for the $2s2p^2\ ^4P_J - 2s^22p\ ^2P^0_{J'}$ intercombination transitions in $Z = 6 - 8$ with other theoretical results and experiment. a) DT. b) Nussbaumer & Storey (1981). c) Lennon et al. (1985). d) Froese Fischer (1994). e) Nussbaumer & Storey (1979). f) Bell et al. (1995). g) Brage et al. (1995). h) CKD. i) Brage et al. (1996). j) MVGK. Experiment by Fang et al. (1993a,b); the experimental uncertainties are given by the quantities in brackets. From the present comparison, a 20% accuracy rating is assigned to the present data

Z	2J	2J′	Pres	Theory	Expt
6	1	1	71.9	42.5^a,55.3^b, 74.4^c, 62.6^d	
	1	3	81.9	40.2^a,65.5^b, 77.8^c, 69.6^d	
	1	1+3	154	82.7^a, 121^b, 152^c, 132^d	146(10)
	3	1	1.87	1.01^a,1.71^b, 1.70^c, 1.44^d	
	3	3	10.2	8.11^a,5.24^b, 12.4^c, 9.43^d	
	3	1+3	12.1	9.12^a,6.95^b, 14.1^c, 10.9^d	12(2)
	5	3	50.3	34.4^a,43.2^b, 53.9^c, 46.1^d	51(4)
7	1	1	418	288^a, 339^e, 347^f, 361^g, 2.69^h	
	1	3	446	270^a, 364^e, 362^f, 372^g, 887^h	
	1	1+3	864	558^a, 703^e, 708^f, 733^g, 890^h	1019(64)
	3	1	11.7	6.95^a,8.95^e, 8.78^f, 9.11^g, 7.88^h	
	3	3	70.0	59.0^a,59.0^e, 60.2^f, 65.1^g, 278^h	
	3	1+3	81.7	66.0^a,68.0^e, 69.0^f, 74.2^g, 286^h	75(6)
	5	3	317	229^a, 251^e, 266^f, 282^g, 550^h	308(22)
8	1	1	1720	1290^a, 931^h, 1470^i, 1810^j	
	1	3	1760	1200^a, 1900^h, 1430^i, 1770^j	
	3	1	48.4	30.9^a, 33.9^h, 38.4^i, 22.8^j	
	3	3	315	276^a, 330^h, 294^i, 328^j	
	5	3	1330	1020^a, 1020^h, 1170^i, 1040^j	